Molecular Pharmacology Fast Forward. Published on June 11, 2009 as doi:10.1124/mol.109.056002
This article has not been copyedited and formatted. The final version may differ from this version.

MOL#56002

Hepatic CYP3A suppression by high concentrations of proteasomal inhibitors: A consequence of endoplasmic reticulum (ER)-stress induction, activation of PERK and GCN2 eIF2α kinases and global translational shut-off.

Poulomi Acharya, Juan C. Engel and Maria Almira Correia.

Departments of Cellular & Molecular Pharmacology (*P.A., M.A.C.*), Pharmaceutical Chemistry (*M.A.C.*), Biopharmaceutical Sciences (*M.A.C.*), and Pathology *(J. C. E.)*, The Liver Center (*P.A., M.A.C.*), and Sandler Center for Basic Research in Parasitic Diseases *(J. C. E.)*, University of California, San Francisco, CA 94158

Molecular Pharmacology Fast Forward. Published on June 11, 2009 as DOI: 10.1124/mol.109.056002
This article has not been copyedited and formatted. The final version may differ from this version.

a). **RUNNING TITLE: CYP3A suppression by proteasomal inhibitors**

b). [§]**Corresponding Author:** M. A. Correia

Dept. of Cellular and Molecular Pharmacology,

Mission Bay Campus, Genentech Hall

600 16th Street, N572F/Box 2280

University of California, San Francisco, CA 94158

415-476-3992 (TEL); 415-476-5292 (FAX)

e-mail: almira.correia@ucsf.edu

c). Number of text pages: 42

Number of figures: 10

Number of References: 37

Abstract: 247 words

Introduction: 748 words

Discussion: 1494 words

d). The abbreviations used are: 4-(2-aminoethyl)benzenesulfonyl fluoride hydrochloride (AEBSF); α-subunit of the eukaryotic initiation factor eIF2 (eIF2α); adenylate kinase (AK); autophagic-lysosomal degradation (ALD); 4,6'-diamidino-2-phenylindole dihydrochloride (DAPI); 3,5-dicarbethoxy-2,6-dimethyl-4-ethyl-1,4-dihydropyridine (DDEP); dexamethasone (Dex); endoplasmic reticulum (ER); ER-associated degradation (ERAD); erythroid HRI (eHRI); general control non-derepressible-2 (GCN2); Heme-regulated inhibitor (HRI); High molecular mass (HMM); Horse radish peroxidase (HRP); IRE-1 inositol requiring/ERN1 (ER to nucleus signaling 1); Madin-Darby canine kidney cells (MDCKC); mouse embryo fibroblasts (MEFs); β-Mercaptoethanol (β-ME); Phenylmethylsulfonyl fluoride (PMSF); PKR-like ER-bound eIF2α-kinase (PERK); RNA-dependent protein kinase (PKR); rat hepatocyte lysate (RHL); tryptophan

Molecular Pharmacology Fast Forward. Published on June 11, 2009 as DOI: 10.1124/mol.109.056002
This article has not been copyedited and formatted. The final version may differ from this version.

2,3 dioxygenase (TDO); Tween 20-Tris-buffered saline (TTBS); unfolded protein response (UPR); ubiquitin (Ub); Ub-mediated 26S proteasomal degradation (UPD).

Molecular Pharmacology Fast Forward. Published on June 11, 2009 as DOI: 10.1124/mol.109.056002
This article has not been copyedited and formatted. The final version may differ from this version.

ABSTRACT:

Hepatic cytochromes P450 3A (CYP3A) are endoplasmic reticulum (ER)-proteins, responsible for xenobiotic metabolism. They are degraded by the ubiquitin-dependent 26S proteasome. Consistent with this, we have shown that proteasomal inhibitors MG132 and MG262 stabilize CYP3A proteins. However, more recently MG132 was reported to suppress CYP3A due to impaired NFκB-activation and consequently reduced CYP3A protein stability. Because MG132 concentration used in those studies was 10-fold higher than that required for CYP3A stabilization, we examined the effect of MG132 (0-300 μM) concentration-dependent proteasomal inhibition on CYP3A turnover in cultured primary rat hepatocytes. We found a biphasic MG132-concentration effect on CYP3A turnover: Stabilization at 5-10 μM with marked suppression at >100 μM. Proteasomal inhibitors reportedly induce ER-stress, heat shock and apoptotic response. Because at these high MG132-concentrations, such CYP3A suppression could be due to ER-stress induction, we monitored the activity of PERK [PKR (RNA-dependent protein kinase)-like ER kinase (EIF2AK3)], the ER-stress-activated eIF2α kinase. Indeed, we found a marked (≈ 4-fold) MG132 concentration-dependent PERK autophosphorylation, along with an 8-fold increase in eIF2α-phosphorylation. In parallel, MG132 also activated GCN2 [general control non-derepressible-2 (EIF2AK4)] eIF2α kinase in a concentration-dependent manner, but not the heme-regulated inhibitor, HRI eIF2α kinase [(EIF2AK1)]. Pulse-chase, immunoprecipitation/immunoblotting analyses documented the consequently dramatic translational shut-off of total hepatic protein including but not limited to CYP3A and tryptophan 2,3-dioxygenase protein syntheses. These findings reveal that at high concentrations, MG132 is indeed cytotoxic and can suppress CYP3A synthesis, a result confirmed by confocal immunofluorescence analyses of MG132-treated hepatocytes.

Molecular Pharmacology Fast Forward. Published on June 11, 2009 as DOI: 10.1124/mol.109.056002
This article has not been copyedited and formatted. The final version may differ from this version.

INTRODUCTION

Hepatic cytochromes P450 (P450s) are endoplasmic reticulum (ER)-anchored integral proteins responsible for the metabolism of various endobiotics as well as xenobiotics, including drugs, toxins and carcinogens. Of these, human liver CYP3A4 and its mammalian orthologs are noteworthy not only because they biotransform a host of clinically relevant drugs, but also because they are inducible by their substrates via enhanced transcriptional/translational activity, or protein stabilization. Such substrate-mediated regulation of hepatic CYP3A[1] content can result in clinically relevant drug-drug interactions (DDIs), respectively prototyped by the DDIs encountered between rifampin-ethinylestradiol cotherapy on one hand, and grapefruit juice furanocoumarins and felodipine cointake, on the other (Yang et al., 2008). The latter was elegantly documented to be due to furanocoumarin-induced suicidal inactivation of intestinal CYP3A4 and subsequent proteolytic degradation (Lown et al., 1997; Paine et al., 2006).

We have previously reported using various selective probes that native and suicidally inactivated hepatic CYPs 3A[1] are turned over via ubiquitin (Ub)-mediated 26S proteasomal degradation (UPD), but not autophagic-lysosomal degradation (ALD), in incubations of freshly isolated hepatocyte suspensions (Wang et al., 1999), cultured primary rat hepatocytes (Faouzi et al., 2007), and *in vitro* reconstituted CYP3A4 ubiquitination-degradation systems (Korsmeyer et al., 1999). Accordingly, treatment of cultured primary rat hepatocytes with the proteasome inhibitor MG132 or MG262 not only resulted in enhanced profiles of ubiquitinated native and suicidally inactivated CYP3A, but also stabilized their hepatic levels (Faouzi et al., 2007). Treatment with the ALD inhibitors, 3-methyladenine and NH_4Cl, on the other hand, had little effect on CYP3A turnover. This was experimentally reiterated in *Saccharomyces cerevisiae* wild type strains and strains with genetic deletions or defects in specific proteins involved in the ER-associated degradation (ERAD) of various integral and luminal ER proteins. Thus, through

Molecular Pharmacology Fast Forward. Published on June 11, 2009 as DOI: 10.1124/mol.109.056002
This article has not been copyedited and formatted. The final version may differ from this version.

these genetic yeast screens, the proteolytic degradation of heterologously expressed CYP3A4 was also shown to subscribe to a bona fide ERAD, dependent on UPD but not the vacuolar (ALD) pathway (Murray and Correia, 2001; Liao et al., 2006).

Several reports have however challenged this conclusion, and have provided evidence that proteasome inhibitors such as MG132 suppress rather than stabilize CYP3A protein. While some reports claimed that this suppression is at the mRNA and protein level (Noreault-Conti et al., 2006), others claimed it was due to NFκB-mediated regulation of CYP3A protein stability (Zangar et al., 2008). Accordingly, evidence was provided for a reduced NFκB activation due to MG132-mediated inhibition of proteasomal function (Zangar et al., 2008). NFκB activation requires unleashing from its inhibitory IκB regulators via proteasomal degradation. These authors documented that MG132-inhibited proteasomal degradation elevated the cellular levels of some IκB inhibitors while maintaining steady-state IκBα levels, thus resulting in a functionally inactive NFκB. This inactive NFκB, the authors proposed, would be incapable of controlling cellular oxidative stress, in turn resulting in CYP3A protein destabilization. Indeed, NAI [(6-amino-4-(4-phenoxyphenyl-ethylamino)quinazoline)], an NFκB activation inhibitor, was shown to exhibit similar, albeit considerably reduced CYP3A4 protein destabilization.

This finding intrigued us primarily because of the 10-fold higher MG132 concentrations (200 μM) used for inhibition of NFκB activation, relative to those (10-20 μM) required for proteasomal inhibition. Although we had used similar high concentrations in incubations of freshly isolated hepatocytes[2] (Wang et al., 1999), we had found that these high concentrations were cytotoxic to cultured primary hepatocytes. Indeed, proteasome inhibitors are known to induce ER-stress and enhance apoptosis (Bush et al., 1997; Nishitoh et al., 2002; Lee et al., 2003; Jiang and Wek, 2005a). Given this possibility, we explored whether the diametrically opposite MG132 effects

Molecular Pharmacology Fast Forward. Published on June 11, 2009 as DOI: 10.1124/mol.109.056002
This article has not been copyedited and formatted. The final version may differ from this version.

observed on CYP3A protein stability could stem from differences in the concentrations employed. We therefore examined the effects of MG132 at concentrations ranging from 0-300 μM in cultured primary rat hepatocytes. Our findings described below reveal that MG132 had a biphasic concentration-dependent effect on immunochemically detectable CYP3A levels in cultured rat hepatocytes: Stabilization of CYP3A at lower concentrations and a marked suppression at higher concentrations. However, we show that this suppression stems from MG132-induced unfolded protein response (UPR) and consequent ER-stress, activation of both PERK [PKR (RNA-dependent protein kinase)-like ER kinase (EIF2AK3)], the resident ER-stress inducible eIF2α kinase, and GCN2 [general control non-derepressible-2 (EIF2AK4)] eIF2α kinase and consequent global suppression of hepatic protein synthesis, and not due to reduced CYP3A protein stability as previously reported (Zangar et al., 2008). These findings once again underscore the essential role of UPD in CYP3A ERAD, as well as the concentrations of the proteasomal inhibitors critical for its documentation. Given the increasing recognition of proteasomal inhibitors as invaluable therapeutic agents, they are clinically relevant.

Molecular Pharmacology Fast Forward. Published on June 11, 2009 as DOI: 10.1124/mol.109.056002
This article has not been copyedited and formatted. The final version may differ from this version.

MATERIALS AND METHODS:

Materials: Common cell culture medium and supplements such as Williams' Medium E (WME), Insulin-Transferrin-Selenium-G (100X), bovine serum albumin (BSA), penicillin/streptomycin, L-glutamine, Liver Digestion Medium and Liver Perfusion Medium were obtained from Invitrogen Life Technologies (Carlsbad, CA). Methionine/cysteine-free WME was prepared by the University of California San Francisco (UCSF) Cell Culture Facility (San Francisco, CA). Collagen type I was prepared from frozen rat tails as per a protocol established by the UCSF Liver Center Cell and Tissue Biology Core Facility. Matrigel™ was obtained from BD Biosciences (Bedford, MA). Petri dishes (60 mm, Permanox®) were purchased from Nalge Nunc International (Rochester, NY). Phenylmethylsulfonyl fluoride (PMSF), E-64, antipain and dexamethasone (Dex) were purchased from Sigma/Aldrich (St. Louis, MO). Sodium vanadate, β-glycerophosphate, and sodium fluoride, were obtained from Fisher Scientific (Fair Lawn, NJ). Leupeptin was purchased from Roche Applied Science (Indianapolis, IN), while aprotinin and pepstatin A, were obtained from MP Biomedicals, LLC. (Solon, OH). Bestatin was obtained from ICN Biomedicals, Inc. (Aurora, OH). AEBSF (4-(2-aminoethyl)benzenesulfonyl fluoride hydrochloride) was purchased from Alexis Biochemicals (Enzo Life Sciences, Inc., San Diego, CA). MG132 [Z-Leu-Leu-Leu-CHO] and MG262 [Z-Leu-Leu-Leu-B$(OH)_2$] were purchased from BostonBiochem (Boston, MA). [^{35}S]-EXPRESS methionine was purchased from Perkin-Elmer Life and Analytical Sciences (Boston, MA). Rabbit polyclonal IgGs were raised commercially against purified recombinant rat hepatic eIF2α kinase (HRI), and purified by Hi-Trap® Protein A-Sepharose affinity chromatography.

Animals: Male Sprague-Dawley rats (4-6 weeks old) were purchased from Simonsen Laboratories (Gilroy, California). Rats were housed at the UCSF Animal Care Facility, fed and given water *ad libitum*, and handled according to IACUC guidelines.

Molecular Pharmacology Fast Forward. Published on June 11, 2009 as DOI: 10.1124/mol.109.056002
This article has not been copyedited and formatted. The final version may differ from this version.

Hepatocyte isolation and culture: Hepatocytes were isolated from male Sprague-Dawley rats by *in situ* liver perfusion with collagenase (liver digest medium) and purified by centrifugal elutriation. Hepatocytes ($3x10^6$) were seeded onto 60 mm Permanox culture dishes pre-coated with type I rat tail collagen. Cells were cultured as described (Han et al., 2005) in Williams E medium containing insulin-transferrin-selenium G, 0.1 μM Dex, 50 U/mL penicillin/streptomycin, 2 mM L-glutamine and 0.1% BSA. Cells were overlaid with 0.25 mg/mL Matrigel 3 h after plating. Cells were maintained for 2 days with a daily change of medium to enable recovery and cell function restoration and then induced with 20 μM Dex for 3 days (LeCluyse et al., 1999). Treatments were carried out on the fifth day of culture. Cells were treated with vehicle (DMSO) or MG132 (0, 5, 10, 20, 50, 100, 200, 300 μM) for 6 h. Cells were harvested in lysis buffer consisting of Tris-HCl (20 mM, pH 7.5), 1% Triton, NaCl (150 mM), 10% glycerol, EDTA (1 mM), EGTA (1 mM), NaF (100 mM), tetrabasic sodium pyrophosphate (10 mM), β-glycerophosphate (17.5 mM), N-ethylmaleimide (5 mM), Na_3VO_4 (1 mM) and protease inhibitors PMSF (1 mM), leupeptin (20 μM), aprotinin (1.5 μM), E-64 (50 μM), pepstatin (10 μM), antipain (10 μM), AEBSF (1 mM), bestatin (60 μM). The cells were lysed using an OMNI™-TH homogenizer and sonicated for 40 sec. Lysates were clarified by sedimentation at maximum speed in a table-top microcentrifuge at 4°C for 15 min. Lysate supernatants were subjected to Western immunoblotting analyses and densitometric quantitation using ImageQuant software (*see below*).

Human hepatocyte cultures: Freshly isolated hepatocytes were obtained from CellzDirect. After a Percoll centrifugation to exclude non-viable cells, they were cultured exactly as described above for cultured rat hepatocytes with rifampicin (15 μM) instead of Dex as the CYP3A4 inducer. On the 5th day of culture, cells were treated with vehicle (DMSO) or MG262

Molecular Pharmacology Fast Forward. Published on June 11, 2009 as DOI: 10.1124/mol.109.056002
This article has not been copyedited and formatted. The final version may differ from this version.

(0- 300 μM) for 6 h, and processed exactly as described above.

Pulse-chase analyses of de novo CYP3A synthesis: Hepatocytes were cultured as described above. On the fifth day of culture, cells were treated at time 0, with increasing concentrations of MG132 before the pulse-chase to determine the rate of *de novo* synthesis of CYP3A after treatment. Five h thereafter, the culture medium was replaced with Met/Cys-free WME for 1 h containing the MG132 (0-300 μM) and pulsed with 20 μCi/mL of Easy-Tag [^{35}S]-EXPRESS for 1 h. Each ^{35}S-labeled plate was then washed twice with ice-cold PBS containing excess Met (10 mM) and Cys (1.4 mM). The [^{35}S]-labeled protein was chased with 10 mM Met/1.4 mM Cys medium. Lysates were prepared as described above. To insure equivalent [^{35}S]-uptake into hepatocytes, the radioactivity of aliquots of the initial lysate was monitored in Ecolume (4 mL) by liquid scintillation spectrometry using a Beckman LS3801 liquid scintillation counter. Aliquots of these lysates were also used for CYP3A immunoprecipitation using 1 mg of lysate protein: 3 mg of goat anti-CYP3A IgG. Immunoprecipitates were subjected to SDS-PAGE on a precast 4-20% gradient gel. Gels were dried before PhosphorImager analyses. Aliquots of immunoprecipitated [^{35}S]CYP3A eluates were also subjected to scintillation counting.

Total hepatic protein [^{35}S]-incorporation: Cold rat liver microsomal protein (10 mg) was added as a protein carrier to ^{35}S-labeled cell lysate protein (1 mg), and the protein precipitated with 10 volumes of 5% H_2SO4 in methanol (v:v) followed by at the least 5 washes with the same solution. Pellets were then washed sequentially with 10 volumes of organic solvents: Once with acetone, thrice with ethanol/ether (3:1, v:v), and then once with 80% methanol in distilled water. The pellets were air-dried in a biosafety cabinet overnight and dissolved in 1 N NaOH (1 mL) by shaking at 60°C for 5 h, and adjusted to pH 7-8 with 2 N HCl, and its protein concentration determined by the biscinchoninic acid assay. Lysate protein (200 μg) was subjected to liquid

Molecular Pharmacology Fast Forward. Published on June 11, 2009 as DOI: 10.1124/mol.109.056002
This article has not been copyedited and formatted. The final version may differ from this version.

scintillation counting for specific radioactivity determination. Total ^{35}S-protein incorporation was calculated as cpm/mg protein/h.

Pulse-chase analyses of CYP3A degradation: When the effect of MG132 on CYP3A degradation rate was monitored, cells were cultured as described above. On the 5th day, cells were incubated in a Met/Cys-free medium for 1 h, then pulsed with ^{35}S-Met/Cys for 1 h and chased with cold Met/Cys along with MG132 (0, 10, 20, 200 and 300 μM). Cells were harvested in the lysis buffer at the time of chase (0-time) and at 3 or 6 h thereafter. Lysates prepared as described above, were used for CYP3A immunoprecipitation using 1 mg of lysate protein:3 mg of goat anti-CYP3A IgG. Immunoprecipitates were subjected to SDS-PAGE on a precast 4-20% gradient gel. Gels were dried before PhosphorImager analyses. Aliquots of immunoprecipitated [^{35}S]CYP3A eluates were also subjected to scintillation counting.

Immunofluorescence staining*:* After MG132 (0, 10, 20, 200 and 300 μM) treatment, cells were fixed in methanol for 15 min at -20°C and incubated for 1 h with 2% nonimmune rabbit serum. This was followed by incubation with goat anti-CYP3A antibody (1:500, v:v) for 1 h at room temperature. After washing with PBS, cells were incubated with Alexa Fluor 488 rabbit anti-goat antibody (1:3000, v:v). Cells were observed with a Zeiss Axiovert 200M, LSM 510 Meta confocal microscope using a 100 X, 1.4 aperture oil objective. Images were collected at 1024x1024 frame resolution with a pinhole of 0.75 Airy. Vectashield mounting medium with DAPI was added to the culture chambers for DNA staining of hepatic nuclei (Vector Laboratories). The relative nuclear diameters of untreated and MG132 (300 μM)-treated cells (N = 20 each) were determined as an index of apoptotic shrinkage induced by MG132 treatment.

Molecular Pharmacology Fast Forward. Published on June 11, 2009 as DOI: 10.1124/mol.109.056002
This article has not been copyedited and formatted. The final version may differ from this version.

Cell viability assay via Trypan Blue exclusion: Cells were mixed with Trypan Blue dye 1:1 (v:v) and counted on a Hemocytometer slide. Triplicate samples of each cell culture were treated with the dye and each counted in four quadrants of the slide (12 values for each concentration of MG132 were used to determine the Mean ± SD). Percentage cell viability was calculated as [(Live cells/Total cells) x 100].

Cytotoxicity analyses: A non-destructive luciferase-based bioluminescence ToxiLight™ assay was used to monitor any cytotoxicity of cultured hepatocytes induced by MG132 (0-300 μM) concentrations over the 6 h treatment relative to basal 0 μM/0 h levels. This assay monitors the release of intracellular adenylate kinase (AK) into the culture medium, expressed as relative luminescence units (RLU) values, wherein the emitted light is directly proportional to the AK activity in the medium. Lysates from untreated cells obtained at 0 h were diluted to the equivalent volume with the cell culture medium and equivalent aliquots used to monitor the total (100%) cellular AK activity available for release into the media. The assay was performed by the manufacturer's instructions exactly as previously described (Han et al., 2005). In parallel, following treatment with either 0 or 200 μM MG132 for 6 h, the medium of some cell cultures was replaced with fresh medium without MG132 and they were similarly monitored at 24 or 48 h after initial treatment to determine the progression of the cytotoxicity, if any.

DNA fragmentation analyses as an apoptotic index: In mammalian cells, proteasome inhibition is associated with UPR, eIF2α kinase activation as well as apoptosis (Jiang and Wek, 2005a). To determine the extent of the apoptosis, internucleosomal DNA fragmentation, a hallmark of apoptosis, was monitored in hepatocytes treated with MG132 (0-300 μM) for 6 h using the "Quick Apoptotic DNA Ladder Kit" (ALX-850-242-KI01) obtained from Enzo Life Sciences exactly as described in the kit instructions. Total chromosomal DNA was extracted

Molecular Pharmacology Fast Forward. Published on June 11, 2009 as DOI: 10.1124/mol.109.056002
This article has not been copyedited and formatted. The final version may differ from this version.

from harvested cells, quantified and DNA (250 μg) from each treatment group subjected to 1.2% agarose gel chromatography in the presence of 0.5 μg/mL ethidium bromide. The ethidium-bromide stained DNA ladders were visualized by UV trans-illumination. The medium of some cell cultures treated with MG132 (200 μM) for 6 h, was replaced with fresh medium without MG132 and monitored after 24 and 48 h as well to enable the determination of any progression of this effect with time.

Immunoblotting analyses: Unless specifically stated otherwise, 5% non-fat milk in 0.1% Tween TBS (TTBS) was used for blocking and to make all primary and secondary antibody dilutions and all immunoblots were developed with the SuperSignal West maximum sensitivity Femto or Pico chemiluminiscent substrate (Product No. 34095) from Pierce (Rockford, IL). Actin immunoblotting analyses were routinely conducted with each lysate to insure equivalent protein loading. However, because of the low abundance of basal hepatic PERK, GCN2 and HRI protein content, the protein amounts required for their detection by the Femto system greatly exceeded those required for the detection of the relatively more abundant actin protein. The immunoblots were therefore loaded on the basis of the protein concentration of each cell lysate, and the data normalized on the basis of the immunoblots from lysates harvested at 0 h. In parallel, smaller aliquots (10 μg protein) of these same SDS-PAGE sample buffer-solubilized cell lysates were subjected to actin immunoblotting analyses to verify that they matched the corresponding BCA-determined protein concentrations.

CYP3A, ubiquitinated cellular protein or CYP3A protein was immunoblotted as described (Correia et al., 2005; Faouzi et al., 2007). eIF2α/eIF2αP, actin, and Grp78/BiP were subjected to immunoblotting analyses as detailed (Han et al., 2005). HRI protein and hepatic cytosolic tryptophan 2,3- dioxygenase (TDO) immunoblotting analyses were carried out with primary

Molecular Pharmacology Fast Forward. Published on June 11, 2009 as DOI: 10.1124/mol.109.056002
This article has not been copyedited and formatted. The final version may differ from this version.

rabbit polyclonal antibodies against the corresponding recombinant rat hepatic HRI and TDO proteins as described (Liao et al., 2007).

PERK: Lysate protein (100 μg) was used for Western immunoblotting. After blocking the membranes were incubated overnight with a primary rabbit polyclonal antibody raised against the N-terminal 21-320 residues of human PERK (Santa Cruz Biotechnology, SC-13073; 1:750, v:v) in 4% milk in TTBS. The blots were washed 5 times with 0.1% TTBS, followed by a secondary goat anti-rabbit IgG-HRP [Santa Cruz Biotechnology, (SC-2004); 1:50,000, v:v] in 4% milk in TTBS.

PERK-P: Immunoblotting analyses were identical to those of PERK except that the blocking solution was made of 1% milk, 1% BSA, 0.05% Tween-20 in PBS and 50 mM NaF (a phosphatase inhibitor). Primary and secondary antibody dilutions were made in this same blocking solution. The primary antibody was a rabbit polyclonal raised against a short amino acid sequence containing phosphorylated Thr 981 of human PERK [Santa Cruz Biotechnology (SC-32577); 1:500, v:v]. All washes were carried out with 0.05% Tween-20 and 50 mM NaF in PBS.

The authenticity of the PERK and PERK-P bands was confirmed by treatment of cultured rat hepatocytes with thapsigargin (5 and 10 μM), a well recognized ER-stress inducer that is known to induce and autoactivate PERK via phosphorylation. Lysates from commercially obtained SK-N-KH neuroblastoma-cells overexpressing recombinant PERK protein [Santa Cruz Biotechnology (SC-2410)] were also included as a positive control.

GCN2: Lysate protein (50 μg) was used for immunoblotting analyses. Membranes were first blocked for 1 h, and then incubated with a primary rabbit polyclonal antibody against C-terminal

Molecular Pharmacology Fast Forward. Published on June 11, 2009 as DOI: 10.1124/mol.109.056002
This article has not been copyedited and formatted. The final version may differ from this version.

residues 1350-1649 of human GCN2 [Santa Cruz Biotechnology (SC-66902); 1:1000, v:v] followed by a goat anti-rabbit HRP-conjugated secondary IgG [Bio-Rad Laboratories (170-6515); 1:30,000, v:v]. The specificity of the commercial anti-GCN2 antibody was confirmed by parallel immunoblotting analyses with a monoclonal antibody raised against a mouse GCN2 carboxy terminal domain and kindly provided by Prof. R. C. Wek. Lysates from commercially obtained HeLa cells overexpressing recombinant GCN2 protein [Santa Cruz Biotechnology (103409)] were also included as a positive control.

PhosphorImager analyses/densitometric quantitation: The immunoprecipitated ^{35}S-CYP3A was solubilized with 60 μL of SDS-PAGE loading buffer containing 5% SDS, 20% glycerol, DTT (50 mM) and 5% β-ME in 50 mM Tris buffer, pH 6.8, boiled for 5 min, and then equivalent aliquots (45 μL) were subjected to SDS-PAGE on 4-20% Tris-HCl gels. The gels were then dried and exposed to PhosphorImaging screens and visualized with a Storm Phosphorimager (GE Healthcare). Direct quantification of the radioactive bands in dried gels was performed by ImageJ (NIH) analyses. Image J was also used for quantification of all the immunoblots.

Statistical analyses: The Kolmogorov-Smirnov test was used to check whether the data followed normal distribution. Experiments were performed in triplicate. Data were compared by analysis of variance. *p* values <0.05 were considered statistically significant.

Molecular Pharmacology Fast Forward. Published on June 11, 2009 as DOI: 10.1124/mol.109.056002
This article has not been copyedited and formatted. The final version may differ from this version.

RESULTS:

Concentration-dependent effects of MG132 on hepatic CYP3A protein content and ubiquitination: Immunoblotting analyses with goat anti-rat liver CYP3A23 IgGs of lysates from cultured hepatocytes revealed that treatment with MG132 (0-300 μM) for 6 h resulted in a biphasic effect on CYP3A protein content monitored at 55 kDa: Stabilization at lower 5-10 μM concentrations, with a marked statistically significant ($p<0.001$) reduction at concentrations above 100 μM (**Fig. 1A**). Corresponding CYP3A immunoprecipitation analyses of these lysates followed by immunoblotting analyses with rabbit anti-Ub IgGs revealed a progressively increased level of CYP3A ubiquitination detectable as a characteristic ladder of high molecular mass species (HMM; >75 kDa) (**Fig. 1B**). This profile intensified at 200 μM MG132 concentrations, before declining thereafter. Parallel immunoblotting analyses of these lysates for total protein ubiquitination revealed a time- and concentration-dependent accumulation of hepatic ubiquitinated proteins, which similarly reached a maximum at 200 μM, before starting to decline (**Fig. 1C**). These results confirm MG132-induced functional inhibition of the 26S proteasome, and indicate that at the lower concentrations, MG132 indeed stabilizes both the parent (55 kDa) and ubiquitinated (HMM) CYP3A proteins. Similar suppression was also observed with CYPs 3A4/3A5 in cultured human hepatocytes treated with MG262 (>100 μM), another proteasomal inhibitor that also stabilizes CYPs 3A (Faouzi et al., 2007) (**Fig. 2**).

Concentration-dependent effects of MG132 on hepatic PERK activation: Because proteasome inhibitors are well-recognized inducers of cellular stress in Madin-Darby canine

Molecular Pharmacology Fast Forward. Published on June 11, 2009 as DOI: 10.1124/mol.109.056002
This article has not been copyedited and formatted. The final version may differ from this version.

kidney cells (MDCKC) as well as mouse embryo fibroblasts (MEFs) (Bush et al, 1997; Jiang and Wek, 2005a), we probed whether high concentrations of MG132 could similarly induce ER-stress in cultured hepatocytes, thereby accounting for the observed CYP3A suppression. We examined the autophosphorylation-mediated activation of PERK, the integral ER-stress inducible eIF2α kinase (Harding et al., 2003), as an ER-stress marker in hepatocytes treated with MG132 (0-300 μM) for 6 h. PERK activation can be monitored via immunoblotting analyses with an antibody that recognizes a specific phosphorylated PERK epitope, and quantified by monitoring the resulting ratios of densitometrically quantified PERK-P (hyperphosphorylated species) to total PERK content determined with an antibody that recognizes both phosphorylated and unphosphorylated PERK species. Progressive PERK autophosphorylation was observed even at the lowest (5 μM) MG132 concentration, progressively increasing at the higher concentrations (**Fig. 3A**). Furthermore, in parallel, total PERK content was also increased, possibly as a result of MG132-inducible ER-stress (**Fig. 3A**). The specificity of the commercial antibodies used for immunoblotting analyses of PERK and PERK-P was validated with the use of two positive controls: Lysates from hepatocytes treated with thapsigargin, an ER-stress inducer, as the positive control for PERK induction/autoactivation, as well as lysates from SK-N-KH neuroblastoma-cells overexpressing recombinant PERK protein (**Fig. 3B**).

Parallel immunoblotting analyses of Grp78/Bip, the luminal ER-chaperone that is an accepted ER-stress marker also revealed a biphasic effect of MG132: A marked 4-5-fold Grp78 protein induction over basal levels at the lower (0-50 μM) concentrations, and a progressive decline thereafter at the >100 μM-concentrations in MG132-treated hepatocytes (**Fig. 3C**). However, even at the highest MG132-concentrations Grp78 content remained somewhat above basal levels.

Molecular Pharmacology Fast Forward. Published on June 11, 2009 as DOI: 10.1124/mol.109.056002
This article has not been copyedited and formatted. The final version may differ from this version.

Concentration-dependent effects of MG132 on other hepatic eIF2α kinases: In MEFs, proteasome inhibition is associated primarily with the activation of GCN2 eIF2α kinase rather than PERK (Jiang and Wek, 2005a). To determine if MG132 had any effects on hepatic GCN2, we monitored its content (**Fig. 4**). Our findings revealed that in addition to activating hepatic PERK (**Fig. 3**), MG132 showed a marked concentration-dependent increase not only of hepatic GCN2 content but also of its autophosphosphorylation, as indicated by the significant appearance of hyperphosphorylated GCN2 species ranging between 150 kDa to <206 kDa (**Fig. 4A**), as observed with an in vitro phosphorylated recombinant mouse GCN2 (Berlanga et al., 1999). The specificity of the commercial antibodies used for immunoblotting analyses of GCN2 was validated with the use of a positive control: Lysates from HeLa-cells overexpressing recombinant GCN2 protein (**Fig. 4B**). Qualitatively similar findings were also obtained with a monoclonal antibody raised against a mouse GCN2 carboxy terminal domain and kindly provided by Prof. R. C. Wek (*not shown*). Densitometric quantitation of these hyperphosphorylated species as a fraction of the total GCN2 revealed that MG132 resulted in a significant autoactivation of hepatic GCN2, that was indeed dramatic at concentrations >50 μM (**Fig. 4A**). Comparison of the data in Figs. 3A and 4A reveal that PERK is activated at lower MG132 concentrations than GCN2, thereby revealing its higher sensitivity to proteasomal inhibition.

By contrast, no such increases were detected in hepatic HRI (**Fig. 4C**), the other heme-regulated eIF2α kinase that is reportedly activated in MEFs by proteasomal inhibition by MG132 or bortezomib (Velcade) (Yerlikaya et al., 2008). Together, these findings in cultured rat hepatocytes indicate that high concentrations of MG132 can activate at the least two hepatic eIF2α kinases.

Molecular Pharmacology Fast Forward. Published on June 11, 2009 as DOI: 10.1124/mol.109.056002
This article has not been copyedited and formatted. The final version may differ from this version.

To determine whether such PERK and GCN2 autophosphorylation was functionally relevant to the liver cell, we monitored their eIF2α kinase activity by examining the levels of phosphorylated eIF2α (eIF2αP) with an antibody that specifically recognizes its phosphorylated epitope relative to total eIF2α content in hepatocytes treated with MG132 (0-300 μM) for 6 h. Our findings revealed a progressive increase in eIF2αP levels relative to unaltered total eIF2α levels with a statistically significant increase in the eIF2αP/eIF2α ratios detected at MG132 concentrations 100-300 μM (**Fig. 5**).

Concentration-dependent effects of MG132 on de novo hepatic total protein and CYP3A synthesis: Because eIF2α-phosphorylation results in translational arrest of protein synthesis, we determined whether this eIF2α-phosphorylation had any physiological relevance to MG132-treated hepatocytes by monitoring their *de novo* hepatic protein synthesis by pulse-chase analyses after treatment for 6 h at the indicated MG132-concentration. Once again, a concentration-dependent inhibition of total hepatic protein synthesis was detected, being particularly marked at the higher 200-300 μM MG132-concentrations tested (**Fig. 6A**). These findings indicated that MG132-induced ER-stress along with PERK and GCN2 activation enhanced eIF2α-phosphorylation, thereby causing a global translational shut-off of hepatic protein. CYP3A immunoprecipitation analyses of these ^{35}S-labeled cell lysates from untreated and MG132-treated hepatocytes followed by SDS-PAGE and PhosphorImager scanning revealed inhibited ^{35}S-incorporation into CYP3A protein that was also particularly marked at the higher 200-300 μM MG132-concentrations (**Fig. 6B**). At the lower (10 and 20 μM) MG132-concentrations, a lesser extent of inhibition was observed (**Fig. 6B**). The presence of HMM ^{35}S-labeled CYP3A species in hepatocytes treated with 0-20 μM MG132-concentrations indicated that although *de novo* CYP3A synthesis does occur, some newly synthesized CYP3A is also subject to ubiquitination and accumulates after proteasomal inhibition (**Fig. 6B**). When these

Molecular Pharmacology Fast Forward. Published on June 11, 2009 as DOI: 10.1124/mol.109.056002
This article has not been copyedited and formatted. The final version may differ from this version.

^{35}S-labeled CYP3A immunoprecipitates were quantified by liquid scintillation counting that would reflect both parent (55 kDa) and HMM species, a concentration-dependent inhibition of *de novo* CYP3A synthesis was observed (**Fig. 6C**). Thus not only is this CYP3A synthesis >90% decreased at the higher 200-300 μM MG132-concentrations, but also significantly reduced even at the lower (10 and 20 μM) concentrations (**Fig. 6C**).

Concentration-dependent effects of MG132 on TDO content in cultured rat hepatocyes: To determine the potential physiological relevance of this global protein suppression, we examined the concomitant effects of MG132 on the content of hepatic cytosolic TDO, the rate-limiting enzyme in hepatic tryptophan catabolism **(Fig. 7)**. This enzyme controls tryptophan flux into serotonergic pathways in the CNS and ANS, and thus is physiologically relevant. Similar concentration-dependent MG132-induced TDO suppression was observed **(Fig. 7).** Together these findings indicate that after 6 h of MG132-treatment, global hepatic protein synthesis, including that of CYP3A, TDO and Grp78, is inhibited in a concentration-dependent manner.

Concentration-dependent effects of MG132 on hepatic total protein and CYP3A degradation: MG132 was previously reported to reduce CYP3A4 protein stability in HepG2 cells due to oxidative stress stemming from a MG132-impaired NFκB activation (Zangar et al, 2008). However, such reduced CYP3A4 protein stability i.e. enhanced degradation, was monitored by immunoblotting analyses. We reasoned that if CYP3A synthesis were being concomitantly inhibited, immunoblotting analyses would not adequately reflect CYP3A degradation. Therefore we monitored CYP3A degradation by pulse-chase analyses. Unlike the studies monitoring *de novo* CYP3A synthesis, in these studies hepatocytes were first pulsed with ^{35}S-Met/Cys for 1 h, and then at the time of chase, treated with MG132 (0, 10, 20, 200 and 300 μM) concentrations. Their degradation was followed at 3 and 8 h after pulse-chase in the

Molecular Pharmacology Fast Forward. Published on June 11, 2009 as DOI: 10.1124/mol.109.056002
This article has not been copyedited and formatted. The final version may differ from this version.

presence of indicated MG132-concentrations. CYP3A immunoprecipitation analyses from lysates obtained at these times points, revealed a time-dependent reduction of ^{35}S-labeled protein in untreated hepatocytes, which was significantly blocked also in a MG132-concentration-dependent manner (**Fig. 8**). Thus, these results reveal that MG132 even at the higher concentrations that significantly block *de novo* hepatic protein and CYP3A syntheses (**Fig. 6**), also blocks the degradation of the ^{35}S-labeled CYP3A fraction synthesized in the absence of any MG132 during the initial hour of the pulse-chase (**Fig. 8**).

Confocal immunofluorescence microscopic (CIFM) analyses of MG132-treated hepatocytes: Cultured hepatocytes treated with MG132 (0, 10, 20, 200 and 300 μM) concentrations were fixed, permeabilized and treated with anti-CYP3A IgGs, followed by an Alexa Fluor 488-conjugated secondary antibody (**Fig. 9**). Abundant CYP3A is detected in MG132-untreated hepatocytes spread throughout the cytosol in the typical ER reticular pattern, consistent with Dex-mediated CYP3A induction (**Fig. 9**). Treatment with MG132 at the lower concentrations (10 and 20 μM) led to some CYP3A accumulation (**Fig. 9**). Furthermore, after the 20 μM-treatment a distinct perinuclear as well as plasma membrane CYP3A relocalization was detected (**Fig. 9**). It is unclear whether this CYP3A at the plasma membrane is intracellularly or extracellularly exposed. By contrast, a marked reduction of hepatic CYP3A levels was observed after a 6 h-treatment at the higher 200-300 μM MG132-concentrations (**Fig. 9**), consistent with a corresponding marked reduction in CYP3A synthesis (**Fig. 6C**) and immunochemically detectable CYP3A protein (**Fig. 1**).

Effects of MG132 on hepatocellular necrosis and apoptosis: The marked suppression of several hepatic proteins, including CYPs 3A, at these relatively high MG132 concentrations, led us to probe whether this suppression stemmed from MG132-induced irreversible hepatocellular

Molecular Pharmacology Fast Forward. Published on June 11, 2009 as DOI: 10.1124/mol.109.056002
This article has not been copyedited and formatted. The final version may differ from this version.

damage and necrosis. Trypan Blue exclusion assays of cells treated with MG132 (0-300 μM) for 6 h showed a minimal non-statistically significant drop in cell viability from 99.8 ± 2.1 for untreated cells to 96.4 ± 4.1% for those treated with the higher MG132 (200 and 300 μM) concentrations (**Fig. 10A**). This loss was normalized to 98.1 ± 4.3% after 24 h following the initial treatment with MG132 (200 μM) for 6 h. When hepatic AK release into the extracellular medium was used as a more sensitive biochemical probe of hepatic cell damage (**Fig. 10B**), ≈ 2% of hepatic AK was detected at MG132 concentrations of 0-20 μM, and this AK release into the medium was slightly increased to <15% after 6 h-treatment with the higher 100-300 μM concentrations (**Fig. 10B**). But this slight extracellular AK spillage was largely abolished when after initial MG132 (200 μM) treatment for 6 h, cells were monitored in the absence of MG132 at 24 h and 48 h (**Fig. 10B**). Together, these results reveal that the hepatic CYP3A suppression observed at the higher MG132 concentrations is not due to irreversible cell damage and/or necrotic cell death.

Proteasomal inhibition with consequent ER-stress induction and enhanced eIF2α phosphorylation is well known to induce apoptosis via induced expression of the transcriptional regulator ATF4 and its target gene CHOP, a proapoptotic transcriptional regulator (Harding et al., 2003; Jiang et al., 2004; Jiang and Wek, 2005a). Fluorescence microscopy with higher contrast/illumination of the DAPI-stained nuclei of cells treated at the higher MG132 (200 and 300 μM) concentrations (**Fig. 9**), revealed some minor chromatin perturbation at 6 h of treatment with 300 μM MG132 (**Supplemental Material, Fig. S3**). However, none of the prototypic morphological hallmarks of apoptosis such as chromatin condensation, collapse or budding and/or nuclear shrinkage or fragmentation (Martelli et al., 2001; Ziegler and Groscurth, 2004) were detected at this time (**Supplemental Material, Fig. S3**). Indeed, measurement of the nuclear diameter in untreated cells and cells treated with MG132 (300 μM) (**Fig. 9**), revealed

Molecular Pharmacology Fast Forward. Published on June 11, 2009 as DOI: 10.1124/mol.109.056002
This article has not been copyedited and formatted. The final version may differ from this version.

comparable values of 2.66 ± 0.23 and 2.63 ± 0.24 μm, respectively. However, when double-stranded DNA extracted from cells treated with MG132 (0-300 μM) concentrations was assayed for internucleosomal fragmentation, another major hallmark of nuclear apoptosis, the characteristic 180- to 200-bp DNA fragment ladder was detected to a limited extent in cells treated with the higher MG132 (100-300 μM) concentrations at 6 h. This MG132 (200 μM)-induced profile largely subsided when cells were cultured for longer periods (24 and 48 h) after removal of MG132 from the medium (**Fig. 10C**). These findings using a more sensitive biochemical index of nuclear apoptosis are entirely consistent with the well-recognized and therapeutically exploited effects of proteasomal inhibitors as inducers of ER-stress-mediated apoptosis (Wagenknecht et al., 2000; Jiang and Wek, 2005a). However, although such signs of MG132-induced apoptosis were observed at earlier times of treatment, they were short-lived and dependent on its presence in the medium.

Molecular Pharmacology Fast Forward. Published on June 11, 2009 as DOI: 10.1124/mol.109.056002
This article has not been copyedited and formatted. The final version may differ from this version.

DISCUSSION:

The above findings clearly document that depending on its specific concentration the proteasome inhibitor MG132 can markedly and simultaneously reduce both hepatic CYP3A synthesis and degradation. Because of their opposing nature, the overall effects on immunochemically detectable hepatic CYP3A levels would depend on which pathway predominates under a given experimental condition. The evidence presented supports a biphasic effect on CYP3A levels monitored by immunoblotting and confocal immunofluorescence analyses. It confirms previous reports (Wang et al., 1999; Faouzi et al., 2007; Szczesna-Skorupa and Kemper, 2008), by clearly documenting that at the lower concentrations, MG132 indeed stabilizes CYP3A content, whether monitored by immunoblotting, immunofluorescence, or pulse-chase coupled with CYP3A immunoprecipitation analyses. However, pulse-chase analyses of CYP3A ^{35}S-labeled *before* MG132 treatment, also indicated that this ^{35}S-labeled CYP3A fraction was stabilized even at the higher MG132 concentrations (**Fig. 8**), when *de novo* CYP3A synthesis is almost completely shut down. This MG132-induced CYP3A stabilization is thus entirely consistent with a classical ERAD process for CYP3A turnover, wherein UPD is its principal proteolytic pathway. Thus, rigorous documentation of MG132-mediated inhibition of hepatic CYP3A UPD and its consequent protein stabilization requires either pulse-chase analyses, or much lower concentrations of proteasome inhibitors, particularly when monitored by immunoblotting analyses.

Similar CYP3A stabilization at MG132 (10 μM) was also recently documented in COS1 and HepG2 cells (Szczesna-Skorupa and Kemper, 2008). Interestingly, in that study as in ours (**Fig. 9**), CYP3A was also found to exhibit perinuclear accumulation and plasma membrane migration after 18 h of MG132-treatment. This ER to plasma membrane migration was apparently dependent on nocodazole-sensitive microtubular network (Szczesna-Skorupa and Kemper, 2008)[3]. The cause for this MG132-elicited cellular P450 relocalization is unclear.

Molecular Pharmacology Fast Forward. Published on June 11, 2009 as DOI: 10.1124/mol.109.056002
This article has not been copyedited and formatted. The final version may differ from this version.

Concomitantly, MG132 treatment of hepatocytes for 6 h also progressively induced ER-stress in a concentration-dependent fashion. This ER-stress was signaled by a marked induction of hepatic PERK eIF2α kinase content and its functional activation via autophosphorylation, along with significantly increased content of the ER stress marker Grp78, particularly obvious at the lower MG132 concentrations (**Fig. 3C**). Additionally, MG132 concentration-dependent induction and autophosphorylation of hepatic GCN2 were also observed (**Fig. 4**). The latter are consistent with a similar proteasome inhibitor-elicited GCN2 autoactivation in MEFs (Jiang and Wek, 2005a). Thus not surprisingly, this dual hepatic PERK and GCN2 autoactivation elicited by progressively increasing MG132 concentrations dramatically enhanced hepatic eIF2α phosphorylation, with consequent global translational arrest of *de novo* hepatic protein syntheses. Accordingly, the *de novo* synthesis of hepatic ER-bound CYP3A and cytosolic TDO were impaired in parallel. Furthermore, the observed biphasic Grp78-profile reveals that such MG132-elicited translational arrest may also have reduced Grp78 content (**Fig. 3C**). Thus in spite of the prevailing ER-stress, the synthesis of this ER-stress marker may also have been significantly impaired at the higher MG132 concentrations. Apparently, at these high MG132 concentrations, the cell is incapable of ushering the full extent of protective, stress-counteractive responses and thus becomes vulnerable to cytotoxic and/or apoptotic signals, as the increased nuclear DNA fragmentation attests[4] (**Fig. 10C**).

Together, our findings account for the profound CYP3A suppression by MG132 at 200 μM concentrations detected by immunoblotting analyses (Zangar et al., 2003; Zangar et al., 2008). They also rationalize the differential CYP3A4 suppression observed over 6 h between treatment with the NFκB activation inhibitor NAI (40%) and that with MG132 plus cycloheximide (75%) (Zangar et al., 2008). Cycloheximide is known to markedly induce eIF2α phosphorylation and to synergize the effects of ER-stress inducers in MEFs (Jiang et al., 2003). Cotreatment with this

Molecular Pharmacology Fast Forward. Published on June 11, 2009 as DOI: 10.1124/mol.109.056002
This article has not been copyedited and formatted. The final version may differ from this version.

protein synthesis inhibitor would thus further aggravate the gravely impaired hepatic protein synthetic capacity and lead to further "CYP3A4" suppression. Clearly, MG132-mediated inhibition of CYP3A protein synthesis occurs[5], is quite significant at high concentrations, and needs to be either obviated or circumvented to unmask its concurrent UPD inhibition, particularly when degradation is monitored via immunoblotting analyses.

Proteasome-inhibitors including MG132 and lactacystin reportedly induce a heat-shock response in MDCKC characterized by induction of ER-chaperones Grp78/BiP, Grp94 and ERp72 and cytosolic Hsp70 chaperones (Bush et al., 1997), rendering the cells thermotolerant to subsequent relatively high heat stimuli. Furthermore, gene expression profiling after treatment with MG132, lactacystin or its β-lactone, revealed that many stress-related genes and transcription factors are induced, with inhibited proteasomal function as their salient common feature (Zimmermann, et al., 2000). Proteasomal inhibition results in cellular overload and consequent accumulation and/or aggregation of proteins otherwise destined for UPD clearance. Not surprisingly, the cell responds to this overload by rapidly shutting down translation of new proteins, thereby acquiring additional time to repair the damage, while conserving energy and nutrients that enable it to cope with the insult.

As discussed, this prompt translational arrest in response to proteasomal inhibition is conveniently martialled through the activation of one or more of the four cellular eIF2α kinases: PERK, GCN2, HRI and PKR (EIF2AK2)[6]. This functional eIF2α kinase activation occurs through autophosphorylation, which in turn enhances the phosphorylation of the α-subunit of eIF2 (eIF2αP). Elevated cellular eIF2αP levels can in turn sequester eIF2B, the guanine nucleotide exchange factor that catalyzes eIF2-GDP to eIF2-GTP recycling required for translational initiation. The consequent reduction of eIF2-GTP levels results in global

Molecular Pharmacology Fast Forward. Published on June 11, 2009 as DOI: 10.1124/mol.109.056002
This article has not been copyedited and formatted. The final version may differ from this version.

translational arrest, allowing cells to conserve important resources and to usher a stress remediation program to repair and/or contain the damage and return to normalcy. Although each of these cellular eIF2α kinases has a primary function specified by the nature of the particular stress or insult, each can also play a backup role, when the protagonist is functionally compromised or genetically knocked out (Jiang & Wek, 2005a). Furthermore, each cell may also determine which specific eIF2α kinase is its primary responder to a particular stress. Thus, MG132 autoactivates/induces both PERK and GCN2 in hepatocytes (**Figs. 3** and **4**), whereas it primarily activates PERK in PC12 cells (Nishitoh et al., 2002), and GCN2 in MEFs (Jiang & Wek, 2005a). Similarly, the proteasome inhibitor PS431 (bortezomib, Velcade) also principally activates PERK in human head and neck squamous cell carcinoma cells (Fribley et al., 2004). More intriguingly, MG132 (50 μM)-treatment of wild type MEFs resulted in eIF2α phosphorylation and inhibition of protein synthesis that was unaffected in $PERK^{-/-}$, $GCN2^{-/-}$ or $PKR^{-/-}$ MEFs but was significantly impaired in $HRI^{-/-}$ (Yerlikaya et al., 2008) leading to the proposal that HRI is the principal eIF2α kinase involved in this response. However, our immunoblotting analyses indicate that MG132-induced proteasomal inhibition failed to affect hepatic HRI (**Fig. 4**), which is otherwise effectively activated in hepatocytes by heme depletion (Han et al., 2005; Liao et al., 2007).

ER-stress mediated activation of PERK, and nutrient deprivation- or UV irradiation-mediated activation of GCN2 in MEFs, result in enhanced activation of the transcription factor NFκB (Jiang et al., 2003; Wek et al., 2006). This NFκB activation is firmly associated with their eIF2α phosphorylation, as it is abolished in $PERK^{-/-}$ and $GCN2^{-/-}$ MEFs. Such stress-mediated NFκB activation apparently involves enhanced NFκB translocation into the nucleus after release from its inhibitory IκB regulators with consequent transcriptional upregulation of gene expression involved in stress-remediation and apoptosis (Jiang et al., 2003). Such NFκB unleashing in UV-

Molecular Pharmacology Fast Forward. Published on June 11, 2009 as DOI: 10.1124/mol.109.056002
This article has not been copyedited and formatted. The final version may differ from this version.

stressed MEFs is primarily due to reduced IκB translation, coupled with normal IκB turnover via phosphorylation and subsequent UPD (Jiang and Wek, 2005b). In ER-stressed MEFs, it is due to UPD-independent IκB dissociation (Wek et al., 2006). Interestingly, inhibition of IκB UPD by MG132 (1 μM) significantly decreased UV-induced but not ER-stress induced NFκB activation (Jiang and Wek, 2005b). By contrast, treatment of HepG2 cells with higher MG132 concentrations (200 μM) effectively suppresses NFκB activation, consistent with unaltered IκBα levels but IKKβ and IκBβ stabilization (Zangar et al., 2008). Intriguingly at this high MG132 concentration, in spite of the marked PERK- and GCN2-activation and attendant eIF2α phosphorylation, hepatic NFκB activation is suppressed, being subordinate largely to MG132 proteasomal inhibition. Thus, although high concentrations of proteasomal inhibitors suppress both hepatic CYP3A content and NFκB activation, our collective findings suggest that these responses apparently stem from two separate cellular effects of these agents and may not be causally related.

We believe that our findings are physiologically and pharmacologically relevant. Some proteasomal inhibitors (i.e. Bortezomib/Velcade) are used clinically as apoptotic inducers for multiple myeloma therapy and are being considered for various other cancers (Nalepa et al., 2006; Voorhees and Orlowski, 2006). Other even more efficacious proteasomal inhibitors are being developed for diverse therapeutic strategies. Through similar protein suppression such drugs could functionally impair hepatic P450s and other drug metabolizing enzymes and consequently result in clinically relevant DDIs in patients possibly already compromised by multiple drug therapy. Furthermore, MG132-induced suppression of hepatic TDO, an enzyme that controls circulating tryptophan levels and thus the CNS/ANS serotonergic tone reveals that these agents can also target physiologically relevant pathways. More importantly, these findings suggest that caution is warranted with their dosage regimens as significant hepatic protein

Molecular Pharmacology Fast Forward. Published on June 11, 2009 as DOI: 10.1124/mol.109.056002
This article has not been copyedited and formatted. The final version may differ from this version.

translational arrest occurs even at 10 μM concentrations (**Fig. 6A**). Depending on the specific proteins slated for translational arrest at this low concentration, various other vital hepatic physiological pathways may also be compromised at otherwise therapeutic concentrations of these drugs.

Acknowledgments:

The authors wish to thank Prof. Ronald C. Wek, Indiana University, for providing a GCN2 antibody used in preliminary studies. They also thank Mr. Ali Naqvi and Ms. Theresa Canavan, UCSF Liver Center Cell and Tissue Biology Core Facility (Dr. J. J. Maher, Director) for hepatocyte isolation and elutriation. We also gratefully acknowledge Dr. Ed LeCluyse and Ms. Rachel Whisnant (CellzDirect) for generously providing the human hepatocytes used in these studies.

Molecular Pharmacology Fast Forward. Published on June 11, 2009 as DOI: 10.1124/mol.109.056002
This article has not been copyedited and formatted. The final version may differ from this version.

REFERENCES:

Berlanga JJ, Santoyo J and De Haro C (1999) Characterization of a mammalian homolog of the GCN2 eukaryotic initiation factor 2alpha kinase. *Eur J Biochem* **265**:754-762.

Bush KT, Goldberg AL and Nigam SK (1997) Proteasome inhibition leads to a heat-shock response, induction of endoplasmic reticulum chaperones, and thermotolerance. *J Biol Chem* **272**:9086-9092.

Correia MA, Sadeghi S and Mundo-Paredes E (2005) Cytochrome P450 ubiquitination: branding for the proteolytic slaughter? *Annu Rev Pharmacol Toxicol* **45**:439-464.

Faouzi S, Medzihradszky KF, Hefner C, Maher JJ and Correia MA (2007) Characterization of the physiological turnover of native and inactivated cytochromes P450 3A in cultured rat hepatocytes: a role for the cytosolic AAA ATPase p97? *Biochemistry* **46**:7793-7803.

Fribley A, Zeng Q and Wang CY (2004) Proteasome inhibitor PS-341 induces apoptosis through induction of endoplasmic reticulum stress-reactive oxygen species in head and neck squamous cell carcinoma cells. *Mol Cell Biol* **24**:9695-9704.

Han XM, Lee G, Hefner C, Maher JJ and Correia MA (2005) Heme-reversible impairment of CYP2B1/2 induction in heme-depleted rat hepatocytes in primary culture: translational control by a hepatic alpha-subunit of the eukaryotic initiation factor kinase? *J Pharmacol Exp Ther* **314**:128-138.

Harding HP, Calfon M, Urano F, Novoa I and Ron D (2002) Transcriptional and translational control in the mammalian unfolded protein response. *Annu Rev Cell Dev Biol* **18**:575-599.

Harding HP, Zhang Y, Zeng H, Novoa I, Lu PD, Calfon M, Sadri N, Yun C, Popko B, Paules R, Stojdl DF, Bell JC, Hettmann T, Leiden JM and Ron D (2003) An integrated stress response regulates amino acid metabolism and resistance to oxidative stress. *Mol Cell* **11**:619-633.

Jiang HY and Wek RC (2005a) Phosphorylation of the alpha-subunit of the eukaryotic initiation

factor-2 (eIF2alpha) reduces protein synthesis and enhances apoptosis in response to proteasome inhibition. *J Biol Chem* **280**:14189-14202.

Jiang HY and Wek RC (2005b) GCN2 phosphorylation of eIF2alpha activates NF-kappaB in response to UV irradiation. *Biochem J* **385**:371-380.

Jiang HY, Wek SA, McGrath BC, Scheuner D, Kaufman RJ, Cavener DR and Wek RC (2003) Phosphorylation of the alpha subunit of eukaryotic initiation factor 2 is required for activation of NF-kappaB in response to diverse cellular stresses. *Mol Cell Biol* **23**:5651-5663.

Jiang HY, Wek SA, McGrath BC, Lu D, Hai T, Harding HP, Wang X, Ron D, Cavener DR and Wek RC (2004) Activating transcription factor 3 is integral to the eukaryotic initiation factor 2 kinase stress response. *Mol Cell Biol* **24**:1365-1377.

Korsmeyer KK, Davoll S, Figueiredo-Pereira ME and Correia MA (1999) Proteolytic degradation of heme-modified hepatic cytochromes P450: A role for phosphorylation, ubiquitination, and the 26S proteasome? *Arch Biochem Biophys* **365**:31-44.

LeCluyse E, Bullock P, Madan A, Carroll K and Parkinson A (1999) Influence of extracellular matrix overlay and medium formulation on the induction of cytochrome P-450 2B enzymes in primary cultures of rat hepatocytes. *Drug Metab Dispos* **27**:909-915.

Lee AH, Iwakoshi NN, Anderson KC and Glimcher LH (2003) Proteasome inhibitors disrupt the unfolded protein response in myeloma cells. *Proc Natl Acad Sci U S A* **100**:9946-9951.

Liao M, Faouzi S, Karyakin A and Correia MA (2006) Endoplasmic reticulum-associated degradation of cytochrome P450 CYP3A4 in Saccharomyces cerevisiae: further characterization of cellular participants and structural determinants. *Mol Pharmacol* **69**:1897-1904.

Liao M, Pabarcus MK, Wang Y, Hefner C, Maltby DA, Medzihradszky KF, Salas-Castillo SP, Yan J, Maher JJ and Correia MA (2007) Impaired dexamethasone-mediated induction of tryptophan 2,3-dioxygenase in heme-deficient rat hepatocytes: translational control by a

hepatic eIF2alpha kinase, the heme-regulated inhibitor. *J Pharmacol Exp Ther* **323**:979-989.

Loeper J, Descatoire V, Maurice M, Beaune P, Belghiti J, Houssin D, Ballet F, Feldmann G, Guengerich FP and Pessayre D (1993) Cytochromes P-450 in human hepatocyte plasma membrane: recognition by several autoantibodies. *Gastroenterology* **104**:203-216.

Lown KS, Bailey DG, Fontana RJ, Janardan SK, Adair CH, Fortlage LA, Brown MB, Guo W and Watkins PB (1997) Grapefruit juice increases felodipine oral availability in humans by decreasing intestinal CYP3A protein expression. *J Clin Invest* **99**:2545-2553.

Martelli AM, Zweyer M, Ochs RL, Tazzari PL, Tabellini G, Narducci P and Bortul R (2001) Nuclear apoptotic changes: an overview. *J Cell Biochem* **82**:634-646.

Murray BP and Correia MA (2001) Ubiquitin-dependent 26S proteasomal pathway: a role in the degradation of native human liver CYP3A4 expressed in Saccharomyces cerevisiae? *Arch Biochem Biophys* **393**:106-116.

Nalepa G, Rolfe M and Harper JW (2006) Drug discovery in the ubiquitin-proteasome system. *Nat Rev Drug Discov* **5**:596-613.

Neve EP and Ingelman-Sundberg M (2000) Molecular basis for the transport of cytochrome P450 2E1 to the plasma membrane. *J Biol Chem* **275**:17130-17135.

Nishitoh H, Matsuzawa A, Tobiume K, Saegusa K, Takeda K, Inoue K, Hori S, Kakizuka A and Ichijo H (2002) ASK1 is essential for endoplasmic reticulum stress-induced neuronal cell death triggered by expanded polyglutamine repeats. *Genes Dev* **16**:1345-1355.

Noreault-Conti TL, Jacobs JM, Trask HW, Wrighton SA, Sinclair JF and Nichols RC (2006) Effect of proteasome inhibition on toxicity and CYP3A23 induction in cultured rat hepatocytes: comparison with arsenite. *Toxicol Appl Pharmacol* **217**:245-251.

Paine MF, Widmer WW, Hart HL, Pusek SN, Beavers KL, Criss AB, Brown SS, Thomas BF and Watkins PB (2006) A furanocoumarin-free grapefruit juice establishes furanocoumarins

as the mediators of the grapefruit juice-felodipine interaction. *Am J Clin Nutr* **83**:1097-1105.

Szczesna-Skorupa E and Kemper B (2008) Proteasome inhibition compromises direct retention of cytochrome P450 2C2 in the endoplasmic reticulum. *Exp Cell Res* **314**:3221-3231.

Voorhees PM and Orlowski RZ (2006) The proteasome and proteasome inhibitors in cancer therapy. *Annu Rev Pharmacol Toxicol* **46**:189-213.

Wagenknecht B, Hermisson M, Groscurth P, Liston P, Krammer PH and Weller M (2000) Proteasome inhibitor-induced apoptosis of glioma cells involves the processing of multiple caspases and cytochrome c release. *J Neurochem* **75**:2288-2297.

Wang HF, Figueiredo Pereira ME and Correia MA (1999) Cytochrome P450 3A degradation in isolated rat hepatocytes: 26S proteasome inhibitors as probes. *Arch Biochem Biophys* **365**:45-53.

Wek RC, Jiang HY and Anthony TG (2006) Coping with stress: eIF2 kinases and translational control. *Biochem Soc Trans* **34**:7-11.

Yang J, Liao M, Shou M, Jamei M, Yeo KR, Tucker GT and Rostami-Hodjegan A (2008) Cytochrome P450 turnover: regulation of synthesis and degradation, methods for determining rates, and implications for the prediction of drug interactions. *Curr Drug Metab* **9**:384-394.

Yerlikaya A, Kimball SR and Stanley BA (2008) Phosphorylation of eIF2alpha in response to 26S proteasome inhibition is mediated by the haem-regulated inhibitor (HRI) kinase. *Biochem J* **412**:579-588.

Zangar RC, Kocarek TA, Shen S, Bollinger N, Dahn MS and Lee DW (2003) Suppression of cytochrome P450 3A protein levels by proteasome inhibitors. *J Pharmacol Exp Ther* **305**:872-879.

Zangar RC, Bollinger N, Verma S, Karin NJ and Lu Y (2008) The nuclear factor-kappa B pathway regulates cytochrome P450 3A4 protein stability. *Mol Pharmacol* **73**:1652-1658.

Ziegler U and Groscurth P (2004) Morphological features of cell death. *News Physiol Sci* **19**:124-128.

Zimmermann J, Erdmann D, Lalande I, Grossenbacher R, Noorani M and Furst P (2000) Proteasome inhibitor induced gene expression profiles reveal overexpression of transcriptional regulators ATF3, GADD153 and MAD1. *Oncogene* **19**:2913-2920.

Molecular Pharmacology Fast Forward. Published on June 11, 2009 as DOI: 10.1124/mol.109.056002
This article has not been copyedited and formatted. The final version may differ from this version.

Footnotes:

These studies were supported by the National Institutes of Health grants [DK26506 and GM44037]. We also acknowledge the UCSF Liver Center Core on Cell and Tissue Biology supported by the National Institute of Digestive Diseases and Kidney Center Grant [P30DK26743].

1. CYP3A or CYPs 3A refer to liver CYPs 3A2, 3A23, 3A18 and 3A9 when the statements are applicable to rats and/or human liver CYP3A4/CYP3A5.

2. Higher concentrations of MG132 were used in these hepatocyte incubations, because being a peptide aldehyde it can be readily quenched by the relatively high GSH concentrations present in these freshly isolated cells.

3. This CYP3A at the plasma membrane was found oriented intracellularly towards the cytosol, rather than extracellularly, as documented for several other P450s (Loeper et al., 1993; Neve and Ingelman-Sundberg, 2000).

4. In this context it is worth noting that proteasomal inhibitor-induced eIF2α phosphorylation is the initial event that results in the suppression of protein translation on the one hand, and on the other, apoptosis via delayed translational reinitiation at upstream open reading frames that result in the enhanced expression of apoptotic bZip regulators such as ATF4, CHOP and ATF3 (Harding et al., 2002; Jiang et al., 2004; Jiang and Wek, 2005a). Thus CYP3A suppression and apoptosis are two distinct manifestations of MG132-induced eIF2α phosphorylation. This is underscored by the much lower MG132 concentrations required to suppress CYP3A synthesis (**Fig. 6C**) than those required to induce DNA fragmentation (**Fig. 10C**).

Molecular Pharmacology Fast Forward. Published on June 11, 2009 as DOI: 10.1124/mol.109.056002
This article has not been copyedited and formatted. The final version may differ from this version.

5. Our results however, do not fully explain the 40% inhibition of protein synthesis observed at a 5 μM MG132 concentration in primary rat hepatocytes (Noreault-Conti et al, 2006). It is unclear whether this discrepancy is due to rat strain differences (Fisher 344) or the fact that in that study, the hepatocytes were plated on Matrigel with no overlay, whereas ours were plated on collagen-coated Permanox plates with a Matrigel overlay. Such hepatocyte sandwich cultures would significantly protect cells from stresses, including oxidative stress due to direct exposure to 95% air. Conceivably, differences in stress predisposition and/or relative ER-stress levels may explain this discrepancy. It is noteworthy however, that in certain cells as little as 0.1 μM MG132 can activate UPR and PERK resulting in eIF2α phosphorylation and consequent inhibition of *de novo* protein synthesis (Jiang and Wek, 2005a; Nishitoh et al., 2002).

6. dsRNA-activated PKR is usually induced by viral inducers or class 1 interferons that were not specifically included in the cell culture, and therefore was not examined.

Molecular Pharmacology Fast Forward. Published on June 11, 2009 as DOI: 10.1124/mol.109.056002
This article has not been copyedited and formatted. The final version may differ from this version.

LEGENDS FOR FIGURES:

Figure 1. Concentration-dependent effects of MG132 on CYP3A content in cultured rat hepatocyes. **A.** Rat hepatocyte cultures were treated with 0-300 μM MG132 as detailed. A representative example of Western immunoblotting analyses of rat hepatocyte lysate (RHL; 15 μg protein) from three separate experiments is shown at the top and the densitometric quantitation of each experiment normalized to the CYP3A content in the corresponding untreated (0 μM MG132) RHL is shown at the bottom. Corresponding RHL-aliquots were used for actin immunoblotting analyses as loading controls. Values represent mean ± SD of at the least 3 separate experiments. Statistically significant differences from the untreated value were observed at $p<0.05$ for the 5 μM, $p<0.05$ for the 20 and 50 μM, and $p<0.001$ for the 100-300 μM MG132-treatments. **B**. Aliquots of each of these RHL were used for CYP3A immunoprecipitation, and subsequent Western immunoblotting analyses of the CYP3A immunoprecipitates with an anti-Ub antibody as detailed (Methods). **C**. Relative ubiquitination of total RHL protein at 0, 3 and 8 h, confirming proteasomal inhibition by MG132.

Figure 2. Concentration-dependent effects of MG262 on CYP3A content in cultured human hepatocyes. Human hepatocyte cultures were treated with 0-300 μM MG262 as detailed. A representative example of Western immunoblotting analyses of human hepatocyte lysate (15 μg protein) is shown at the top, with corresponding aliquots used for actin immunoblotting analyses as loading controls. Aliquots of the lysate (1 mg protein) were used for CYP3A immunoprecipitation, and subsequent Western immunoblotting analyses of the CYP3A immunoprecipitates with an anti-Ub antibody as detailed (Methods). Densitometric quantitation of CYP3A content in hepatocytes treated at various MG262 concentrations relative to basal (1.0) value at 0 μM was as follows: 1.20 (5 μM), 0.92 (10 μM), 0.93 (20 μM), 0.67 (50 μM), 0.77 (100 μM), 0.75 (200 μM) and 0.52 (300 μM).

Figure 3. Concentration-dependent effects of MG132 on induction of PERK content and its autophosphorylation in cultured rat hepatocyes. **A.** Rat hepatocyte cultures were treated with 0-300 μM MG132 as detailed. A representative example of Western immunoblotting analyses of RHL from three separate experiments is shown at the top with corresponding aliquots used for actin immunoblotting analyses as loading controls. The densitometric quantitation of the relative PERK-P content (solid bars) to the total PERK immunochemically detectable content (open bars) in each experiment is shown at the bottom. Values represent mean ± SD of at the least 3 separate experiments. Statistically significant differences in PERK-P content and the PERK-P/PERK values were observed at $p<0.05$ for the 20-300 μM MG132-treatments. **B.** The specificity of the anti-PERK and anti-PERK-P antibodies was verified by immunoblotting analyses against lysates from SK-N-SH human neuroblastoma cells overexpressing PERK (400 ng PERK protein) and lysates (50 μg) from hepatocytes treated with thapsigargin (5 or 10 μM), a well-known ER-stress inducer, as positive controls in immunoblotting analyses of lysates (100 μg protein) from hepatocytes treated with 0 or 200 μM MG132 as detailed above (**A**). In parallel, smaller aliquots (10 μg protein) of these same SDS-PAGE sample buffer-solubilized cell lysates were subjected to actin immunoblotting analyses. **C.** RHL aliquots (50 μg protein) were also used for monitoring Grp78/BiP immunochemically detectable content. A representative example of Grp78 Western immunoblotting analyses of RHL from three separate experiments is shown at the top, with corresponding aliquots used for actin immunoblotting analyses as loading controls. The densitometric quantitation of the immunochemically detectable Grp78 content in each experiment is shown at the bottom. Values represent mean ± SD of at the least 3 separate experiments. Statistically significant increases over the basal (untreated) content were observed at $p<0.05$ for 5-200 μM MG132-treatments.

Molecular Pharmacology Fast Forward. Published on June 11, 2009 as DOI: 10.1124/mol.109.056002
This article has not been copyedited and formatted. The final version may differ from this version.

Figure 4. Concentration-dependent effects of MG132 on induction of GCN2 content and HRI content and/or their autophosphorylation in cultured rat hepatocyes. **A.** Rat hepatocyte cultures were treated with 0-300 μM MG132 as detailed. A representative example of Western immunoblotting analyses of RHL from three separate experiments *(the same SDS-PAGE buffer solubilized RHL used for PERK immunoblotting analyses in Fig. 3A)* is shown at the top along with corresponding aliquots used for actin immunoblotting analyses as loading controls. The densitometric quantitation of the relative GCN2-P content (solid bars; hyperphosphorylated forms ranging from 150 to 206 kDa) to the total immunochemically detectable GCN2 content (open bars) in each experiment is shown at the bottom. Values represent mean ± SD of at the least 3 separate experiments. Statistically significant differences in GCN2-P content and the GCN2-P/GCN2 values were observed at $p<0.05$ for the 20-300 μM and 50-300 μM MG132-treatments, respectively. **B.** The specificity of the anti-GCN2 antibodies was verified against lysates (250 ng GCN2 protein) from HeLa cells (CL) overexpressing GCN2, in immunoblotting analyses of lysates (50 μg protein) from hepatocytes treated with 0, 200 or 300 μM MG132 as detailed above (**A**). **C.** Rat hepatocyte cultures were treated with 0-300 μM MG132 as detailed. A representative example of Western immunoblotting analyses of RHL (50 μg protein) from two separate experiments is shown at the top with corresponding aliquots used for actin immunoblotting analyses as loading controls. The densitometric quantitation of the HRI content (band ≈ 76 kDa) is shown at the bottom, as an average value obtained from 2 separate experiments. Phosphorylated HRI is usually observed at 92 kDa. No bands above 76 kDa were observed in these immunoblots.

Figure 5. Concentration-dependent effects of MG132 on eIF2αP content relative to the total hepatic eIF2α content in cultured rat hepatocyes. Rat hepatocyte cultures were treated with 0-300 μM MG132 as detailed. A representative example of Western immunoblotting

analyses of RHL (10 μg protein) from three separate experiments is shown at the top, with actin used as a protein loading control. The densitometric quantitation of the relative eIF2αP/total eIF2α content in each experiment is shown at the bottom. Values represent the mean ± SD derived from the same individual experiments depicted in Figs. 1, 3-5. Statistically significant differences in the eIF2αP/total eIF2α ratios were observed at $p<0.05$ for the 10-50 μM and at $p<0.001$ for the 100-300 μM MG132-treatments.

Figure 6. Concentration-dependent effects of MG132 on de novo total protein and CYP3A syntheses in cultured rat hepatocyes. **A**. Rat hepatocyte cultures were treated with 0, 10, 20, 200 and 300 μM MG132 as detailed. Pulse-chase analyses to monitor *de novo* total protein synthesis at each concentration was carried out as detailed (Methods). Values are depicted as mean ± SD from at the least 3 separate experiments, and expressed relative to the basal rate observed in the corresponding untreated (0 μM MG132) RHL. Statistically significant differences were observed at $p<0.05$ for the MG132 (10 and 20 μM)-treated RHL, and at $p<0.001$ for the MG132 (200 and 300 μM)-treated RHL. **B**. Aliquots from the corresponding pulse-chased RHL (**B**) were used for CYP3A immunoprecipitation analyses. A representative PhosphorImager scan of corresponding aliquots subjected to SDS-PAGE are shown. **C**. Quantitation of ^{35}S-incorporated into CYP3A-immunoprecipitates per h is shown. Values depicted are mean ± SD from at the least 3 separate experiments, and expressed relative to the basal rate observed in the CYP3A-immunoprecipitate from the corresponding untreated (0 μM MG132) RHL. Statistically significant differences from basal value were observed at $p<0.05$ for the CYP3A-immunoprecipitate from MG132 (10 and 20 μM)-treated RHL, and at $p<0.001$ for the CYP3A-immunoprecipitate from MG132 (200 and 300 μM)-treated RHL.

Molecular Pharmacology Fast Forward. Published on June 11, 2009 as DOI: 10.1124/mol.109.056002
This article has not been copyedited and formatted. The final version may differ from this version.

Figure 7. Concentration-dependent effects of MG132 on hepatic TDO content. Aliquots of lysates (20 μg protein) from hepatocytes treated with 0, 10, 20, 50, 100, 200 and 300 μM MG132 along with a purified recombinant rat liver TDO (1 pg protein) as a standard (STD) were also subjected to immunoblotting analyses with rabbit polyclonal anti-TDO IgGs as detailed (Liao et al., 2007). Corresponding aliquots were used for actin immunoblotting analyses as loading controls. Values at 0, 10 and 200 μM MG132-concentrations represent mean ± SD of 3 individual RHL.

Figure 8. Concentration-dependent effects of MG132 on CYP3A protein degradation by pulse-chase analyses in cultured rat hepatocyes. Rat hepatocyte cultures were treated with 0, 10, 20, 200 and 300 μM MG132 for 0, 3 or 8 h after pulse-chase analyses to monitor CYP3A degradation at each concentration as detailed (Methods). Aliquots from the corresponding pulse-chased RHL were used for CYP3A immunoprecipitation analyses. Aliquots of CYP3A-immunoprecipitates were quantified for ^{35}S-radioactivity remaining at 3 or 8 h after treatment at each MG132 concentration. Values depicted are mean ± SD from at the least 3 separate experiments, and expressed relative to the basal value observed in the CYP3A-immunoprecipitate from the corresponding untreated (0 μM MG132) RHL at 0 h. Statistically significant differences from basal 0 h-value were observed at $p<0.05$ for the CYP3A-immunoprecipitates from RHL treated with MG132 (20, 200 and 300 μM) for 8 h.

Figure 9. Confocal immunofluorescence CYP3A protein analyses of cultured rat hepatocyes treated with MG132. Rat hepatocyte cultures were treated with 0, 10, 20, 200 and 300 μM MG132 for 8 h. After crosslinking, treated and untreated rat hepatocyte cultures were fixed and simultaneously stained with antibodies to CYP3A (green) and DAPI-stain for nuclei (blue). Data including the superimposed images from a representative experiment show CYP

Molecular Pharmacology Fast Forward. Published on June 11, 2009 as DOI: 10.1124/mol.109.056002
This article has not been copyedited and formatted. The final version may differ from this version.

3A accumulation at 10 μM, and perinuclear/plasma membrane relocalization at 20 μM. A low-grade diffuse green signal throughout the cell body reveals marked loss of CYP3A protein at 200 and 300 μM concentrations. Higher magnification of these panels is shown in Supplemental Figure S3.

Figure 10. MG132 effects on cell viability, extracellular AK release and hepatic DNA fragmentation in cultured hepatocytes. **A.** Hepatocytes were treated with MG132 for 6 h as detailed and their viability was assessed by the Trypan Blue exclusion assay as described (Methods). Untreated and MG132 (200 μM)-treated hepatocytes were also examined after 24 and 48 h from the initiation of the treatment, but after MG132 withdrawal at 6 h. Data shown are the mean ± SD of triplicate samples. There was no statistically significant difference in cell viability between the untreated and MG132-treated cells. **B.** Corresponding AK release into the culture medium was assayed by the ToxiLight™ Assay kit as described (Methods). Values represent Mean ± SD of three separate cell cultures each treated with the indicated MG132 concentration. **C**. Total nuclear DNA was extracted and subjected to agarose gel chromatography in the presence of ethidium bromide as described (Methods). A DNA ladder was included in parallel as a standard. A representative of one experiment conducted after MG132 (0-300 μM) treatment of hepatocytes for 6 h is shown. Similar analyses of DNA extracted from cells harvested at 24 and 48 h after initial 6 h-treatment with MG132 (200 μM) are also shown.

Figure 1A

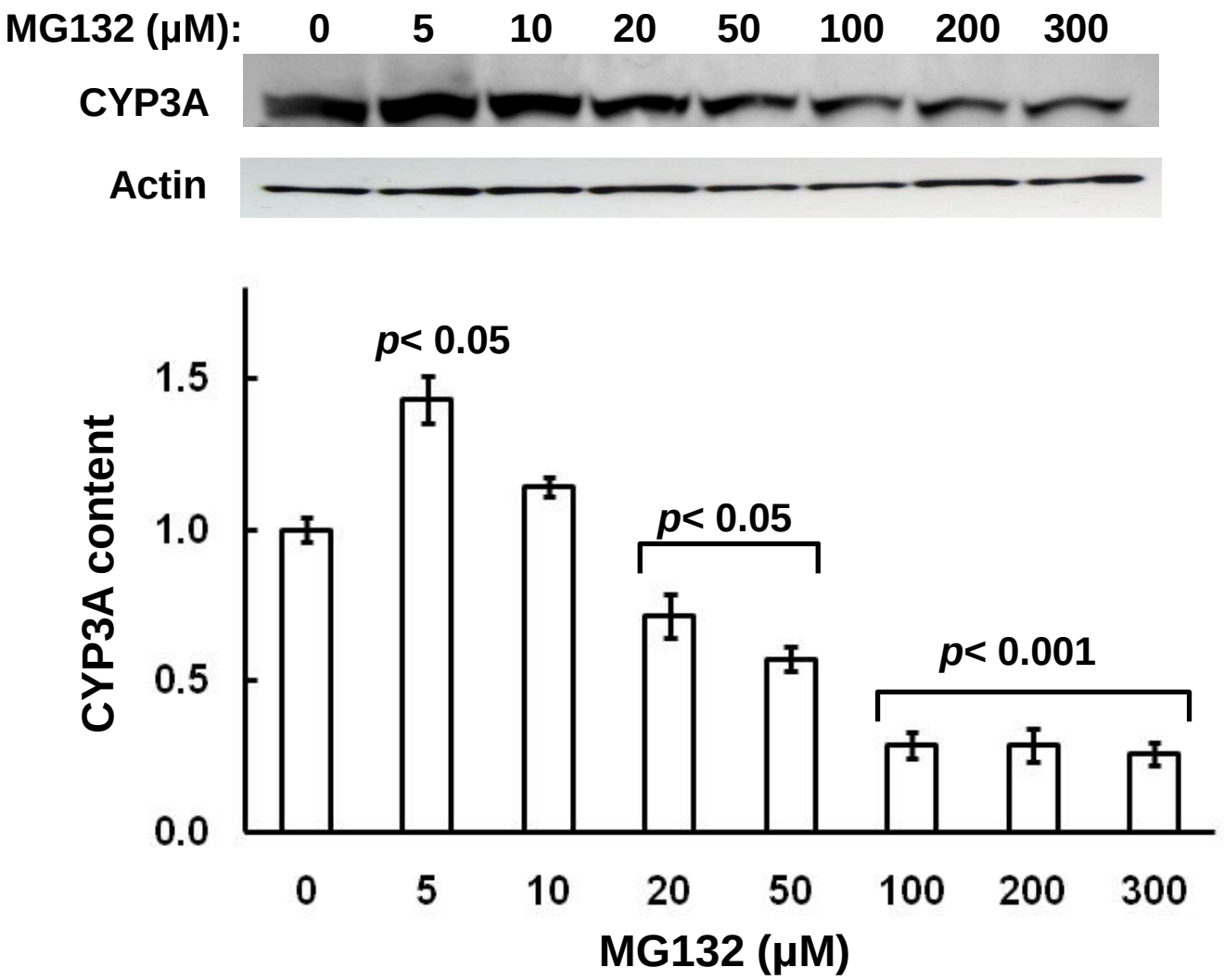

Figure 1B

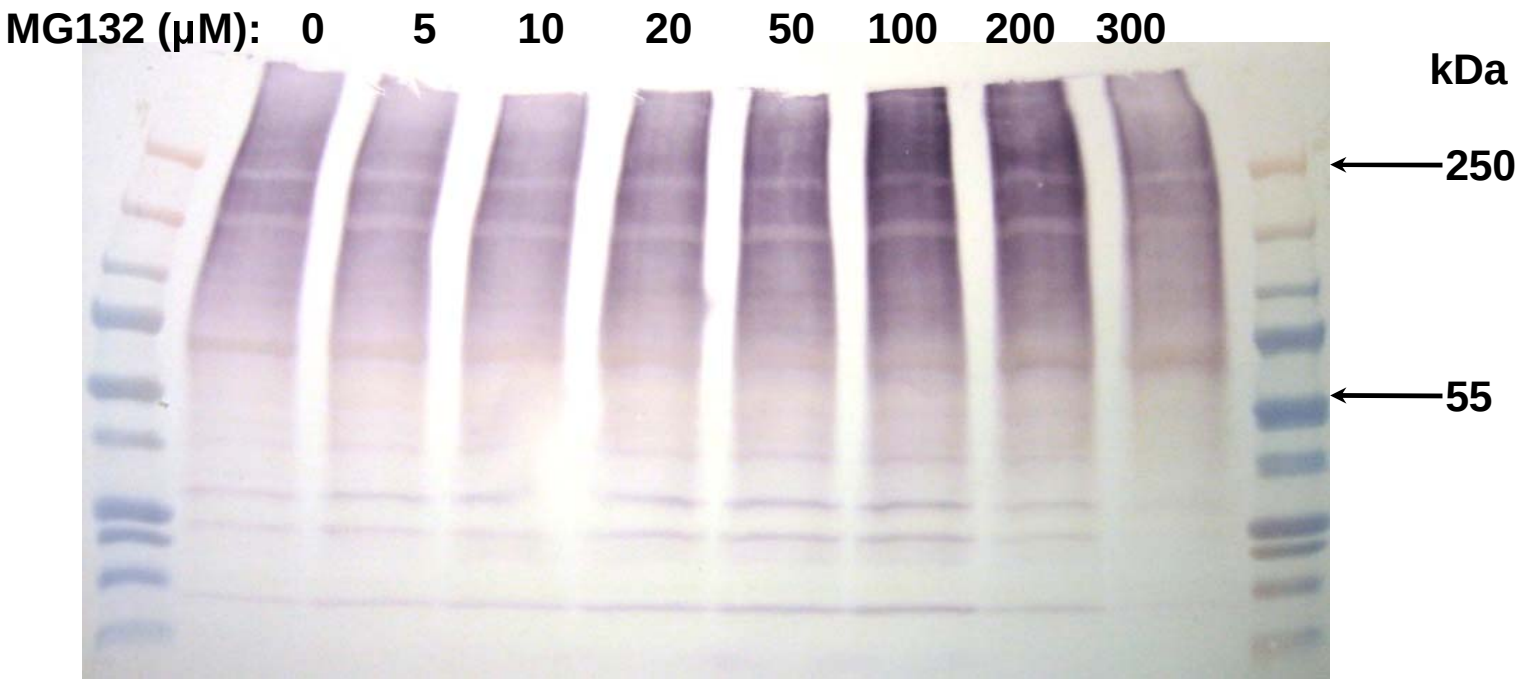

Figure 1C

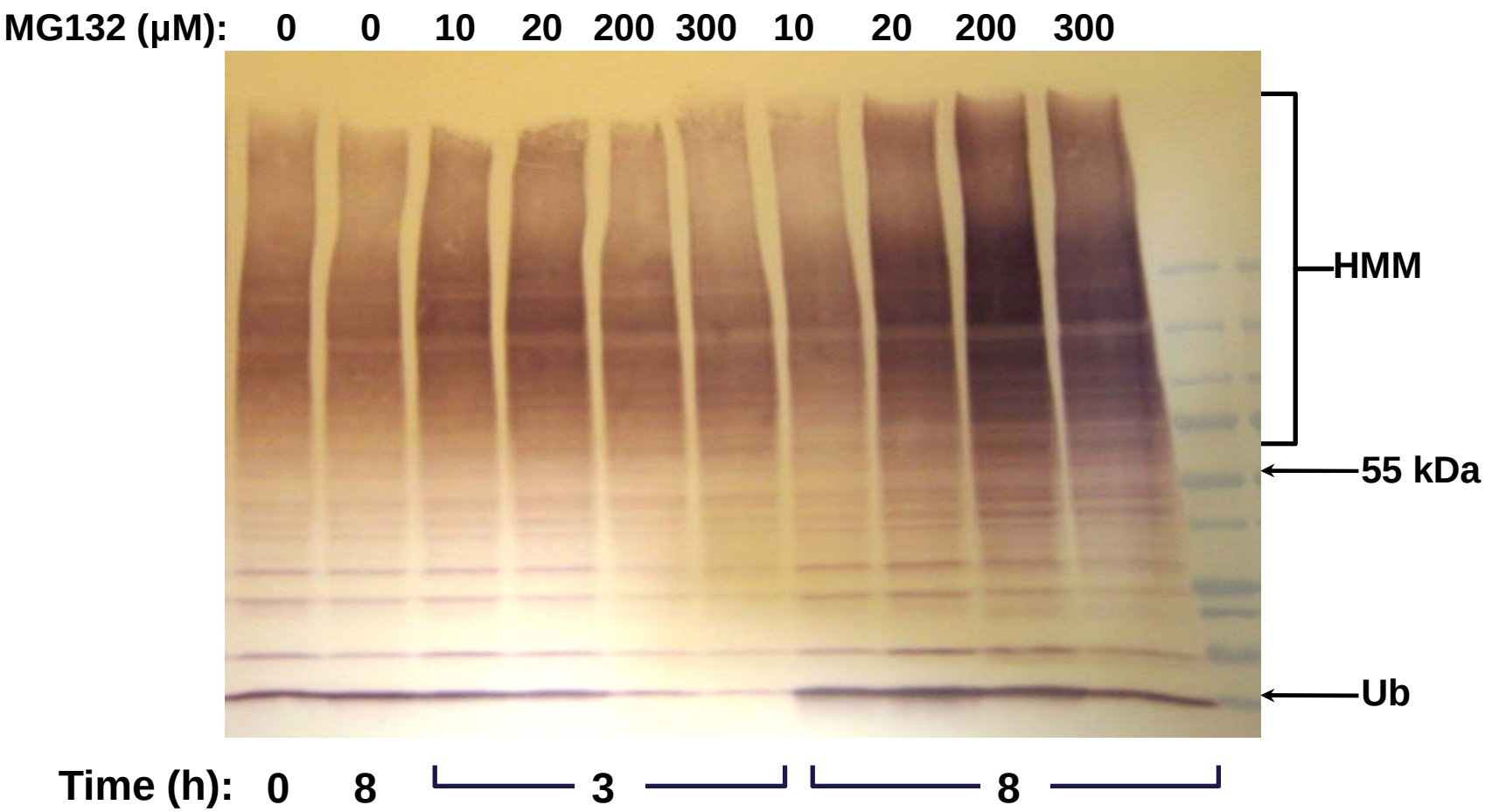

Figure 2

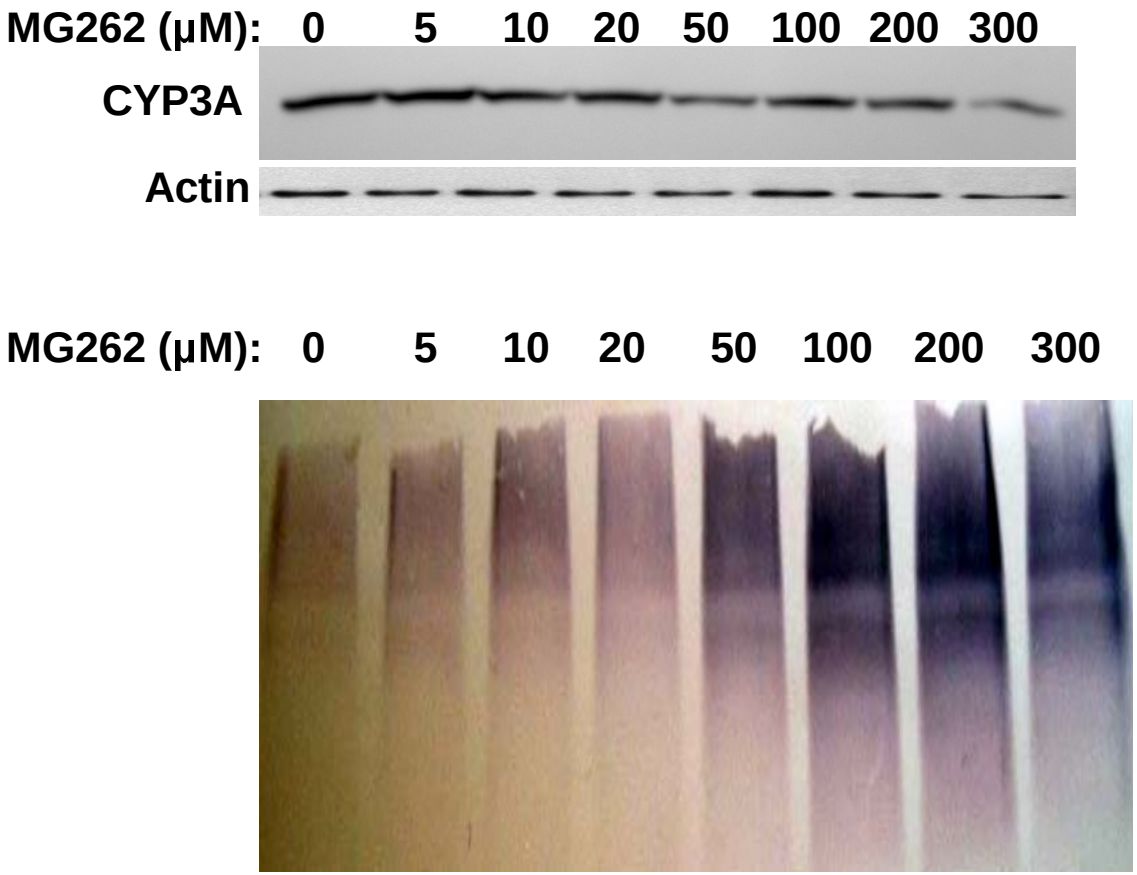

Figure 3A

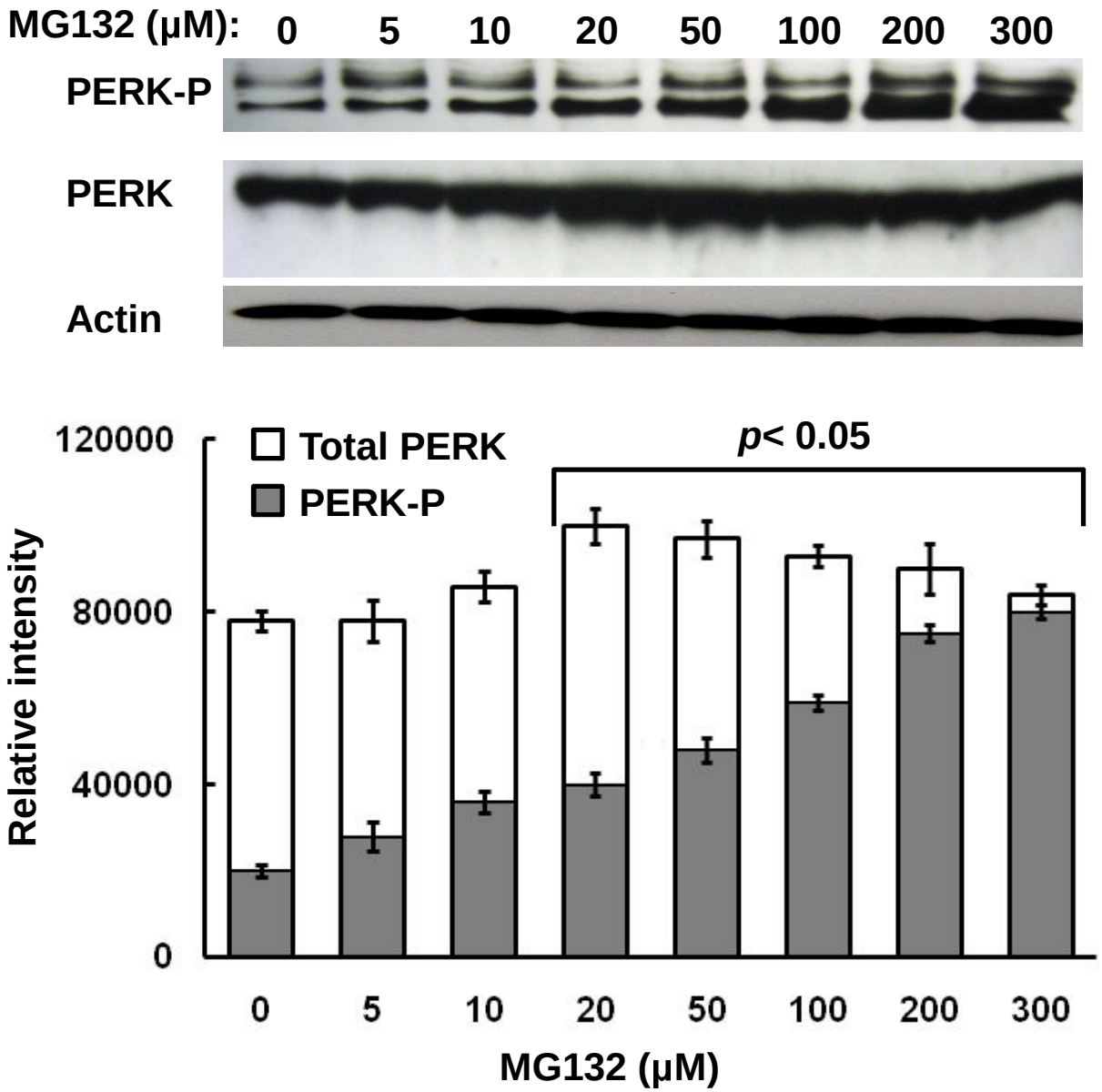

Molecular Pharmacology Fast Forward. Published on June 11, 2009 as DOI: 10.1124/mol.109.056002
This article has not been copyedited and formatted. The final version may differ from this version.

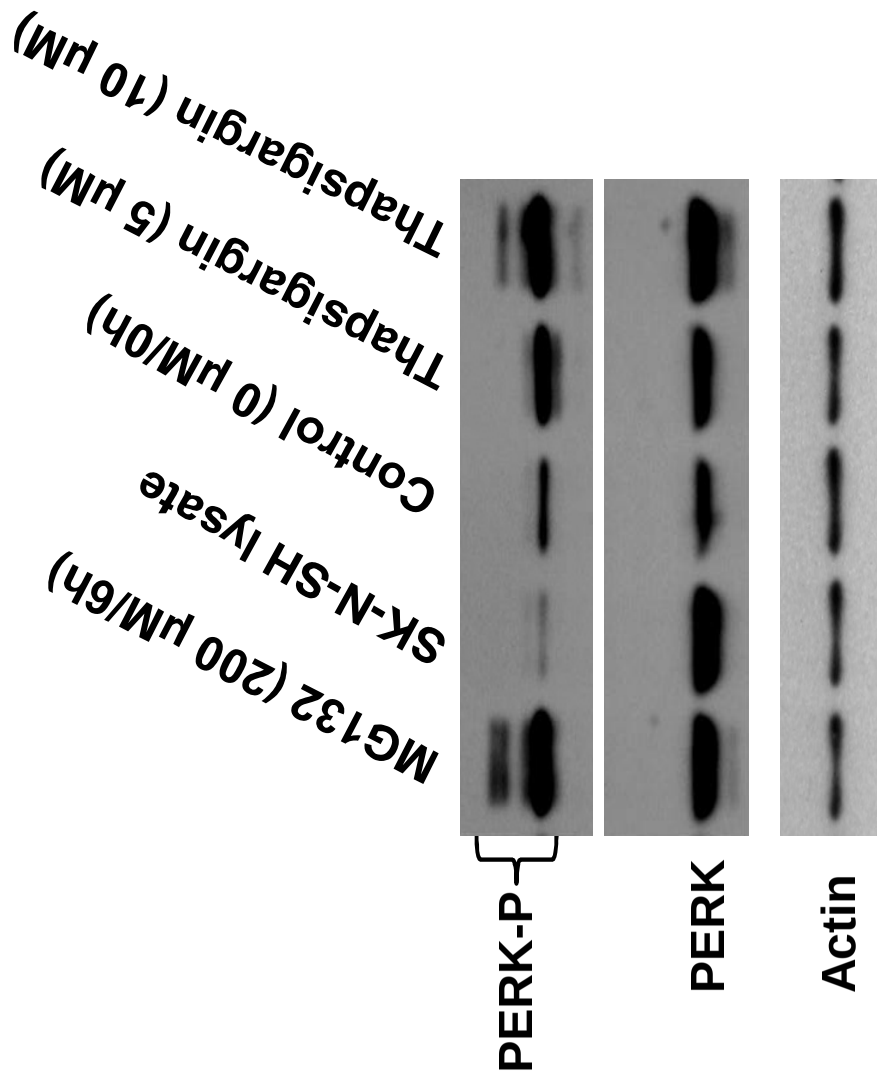

Figure 3B.

Figure 3C

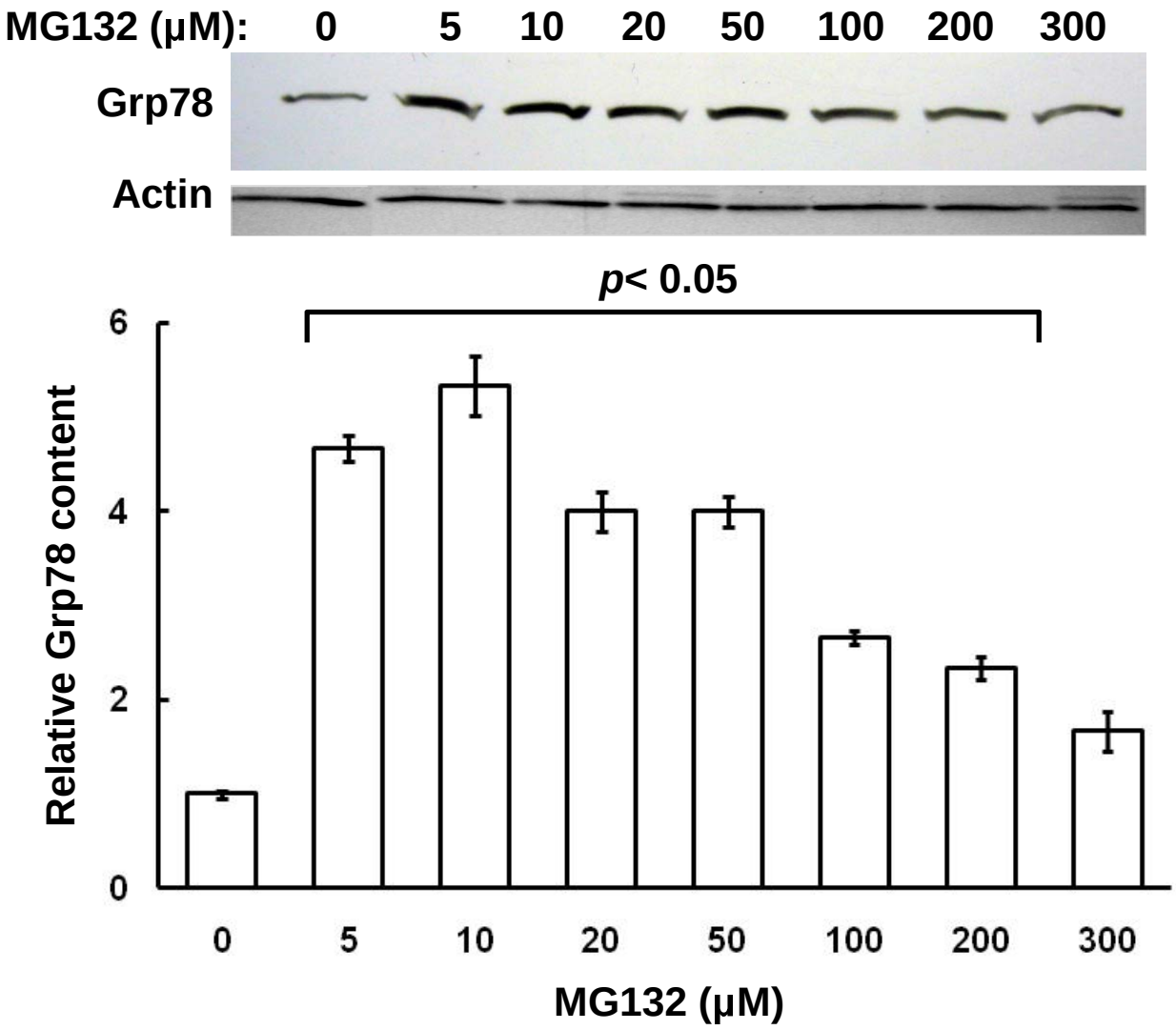

Figure 4A

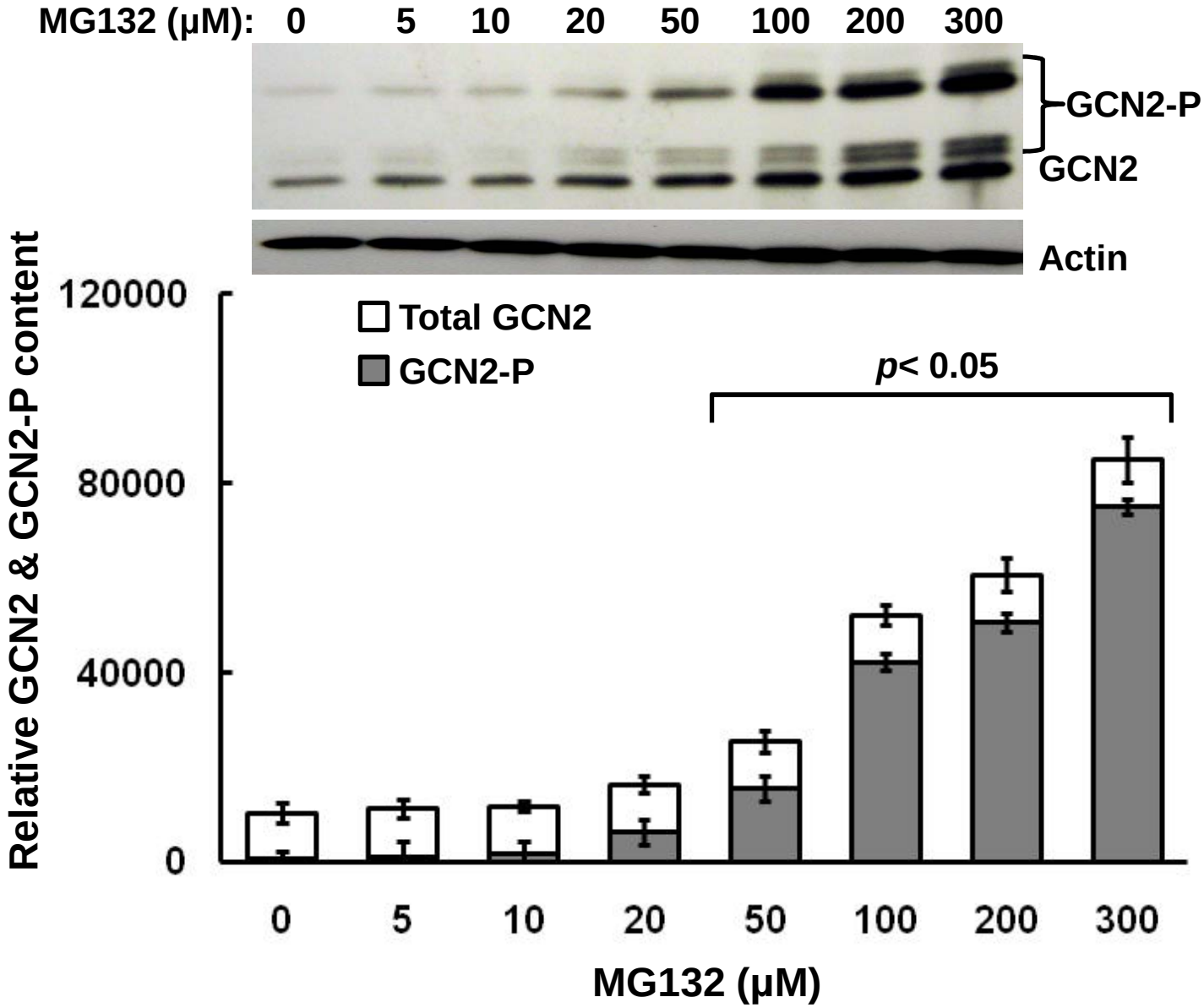

Molecular Pharmacology Fast Forward. Published on June 11, 2009 as DOI: 10.1124/mol.109.056002
This article has not been copyedited and formatted. The final version may differ from this version.

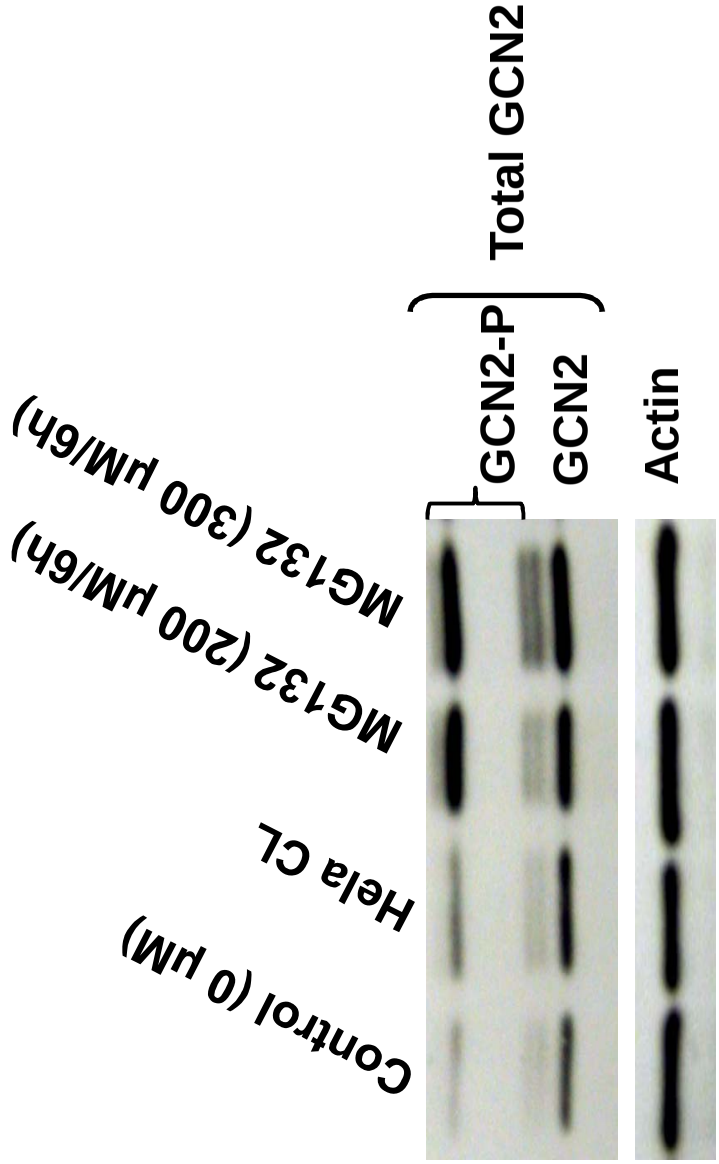

Figure 4B

Figure 4C

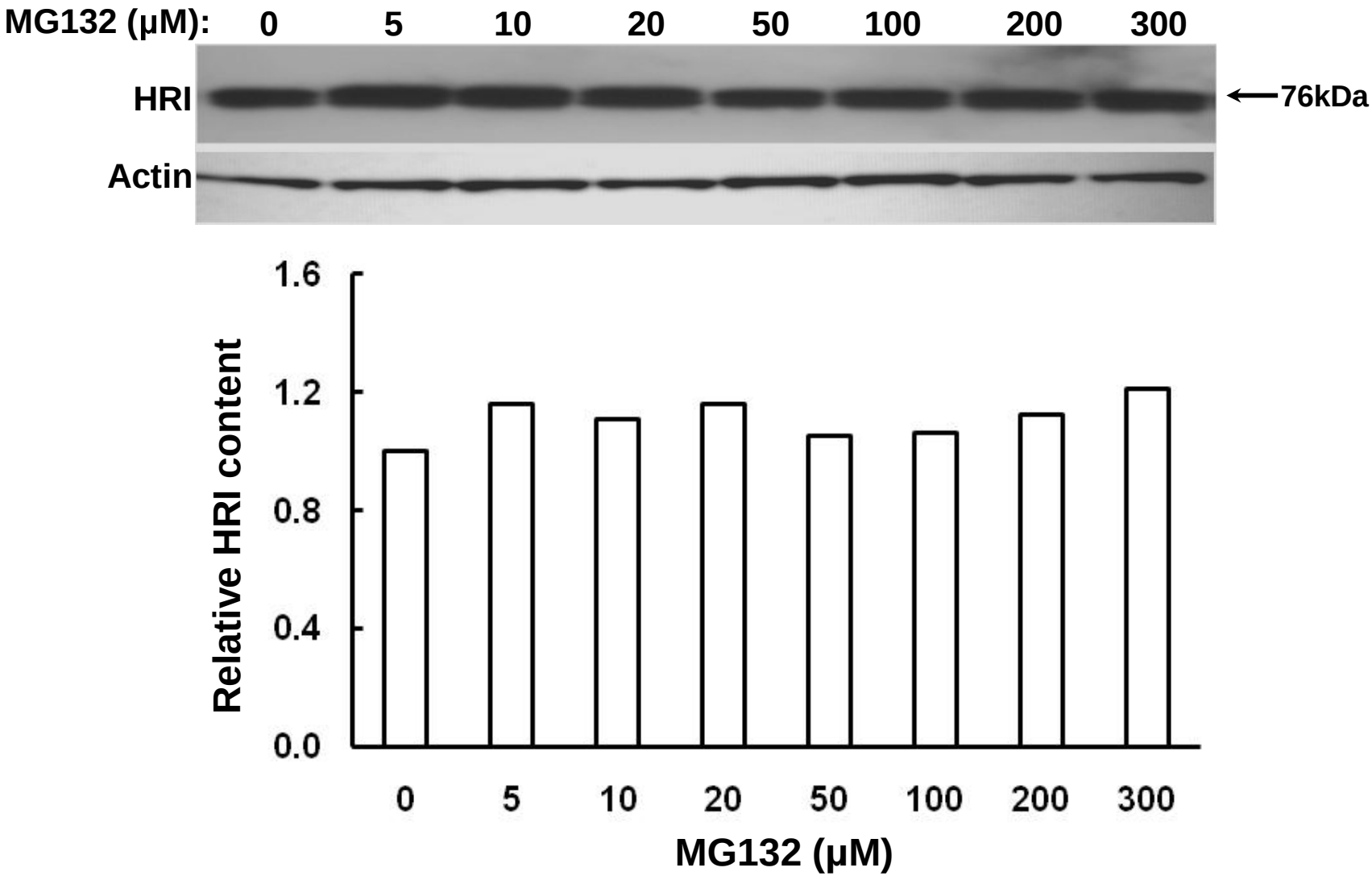

Figure 5

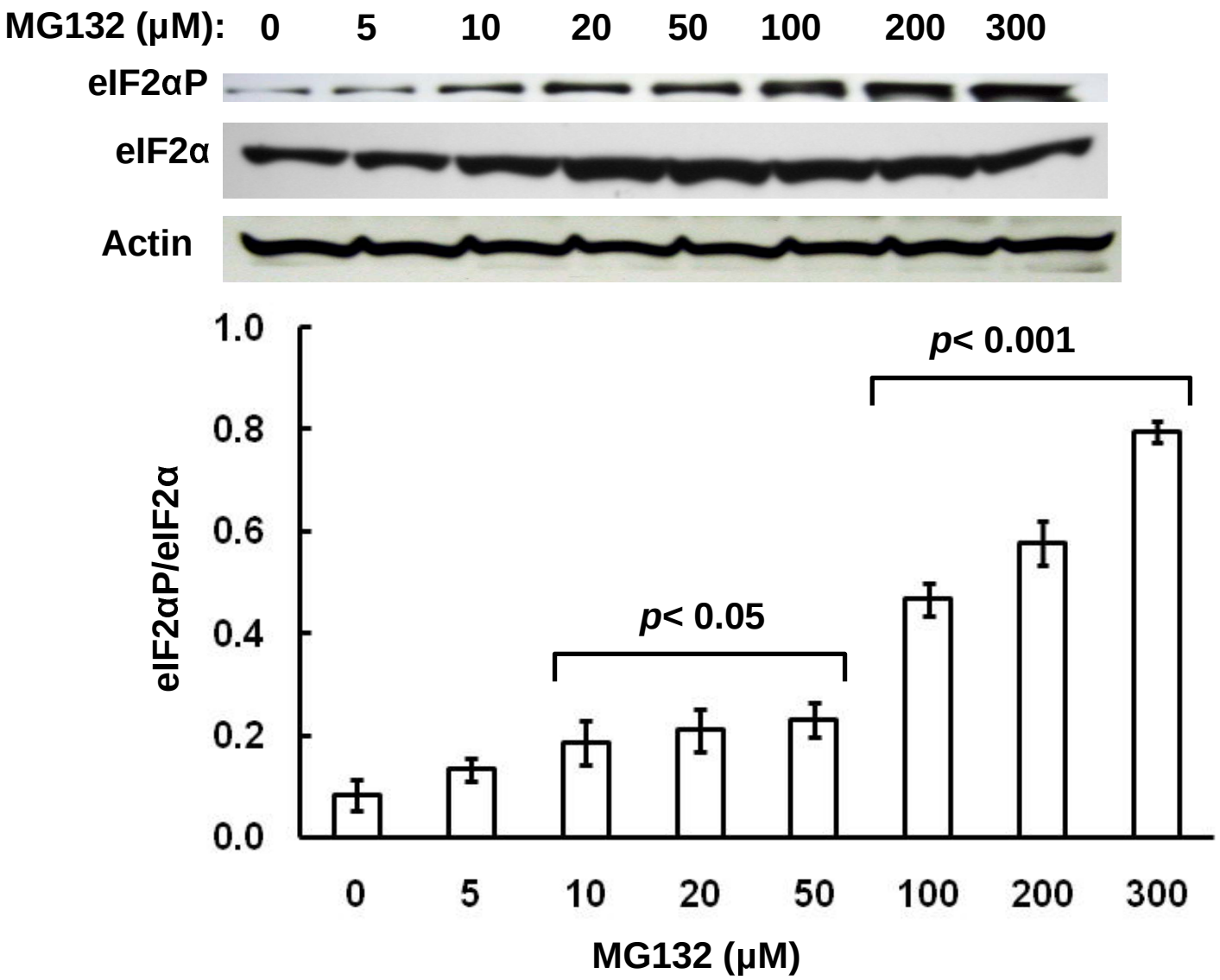

Figure 6A

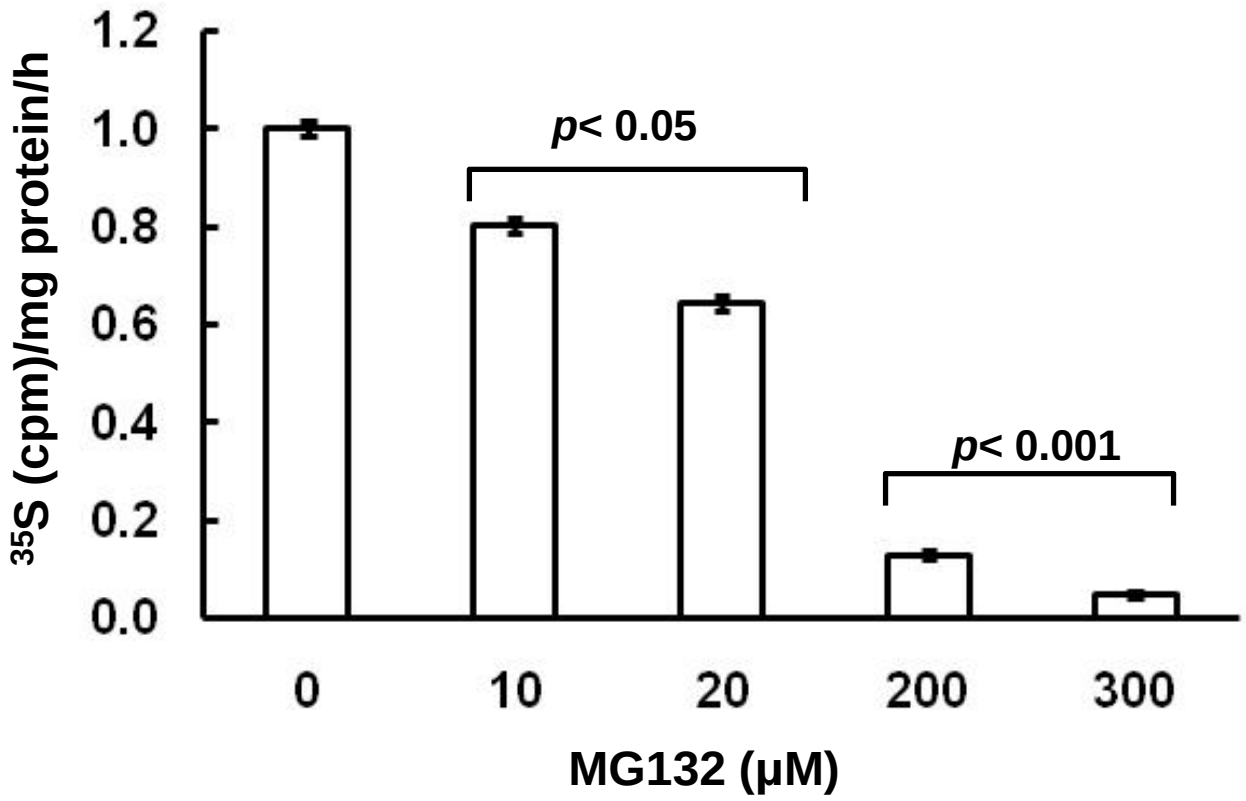

Figure 6B

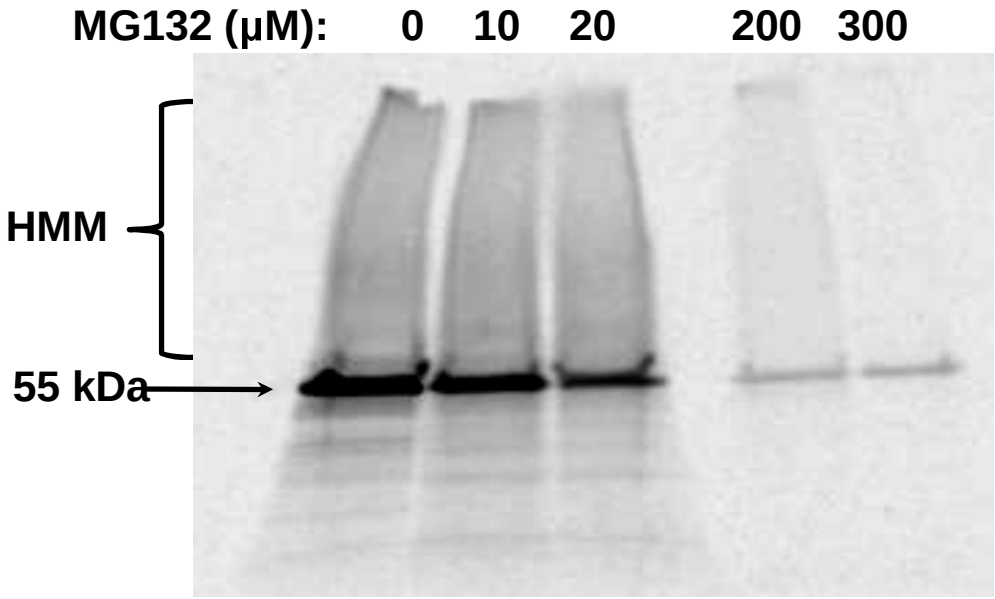

Figure 6C

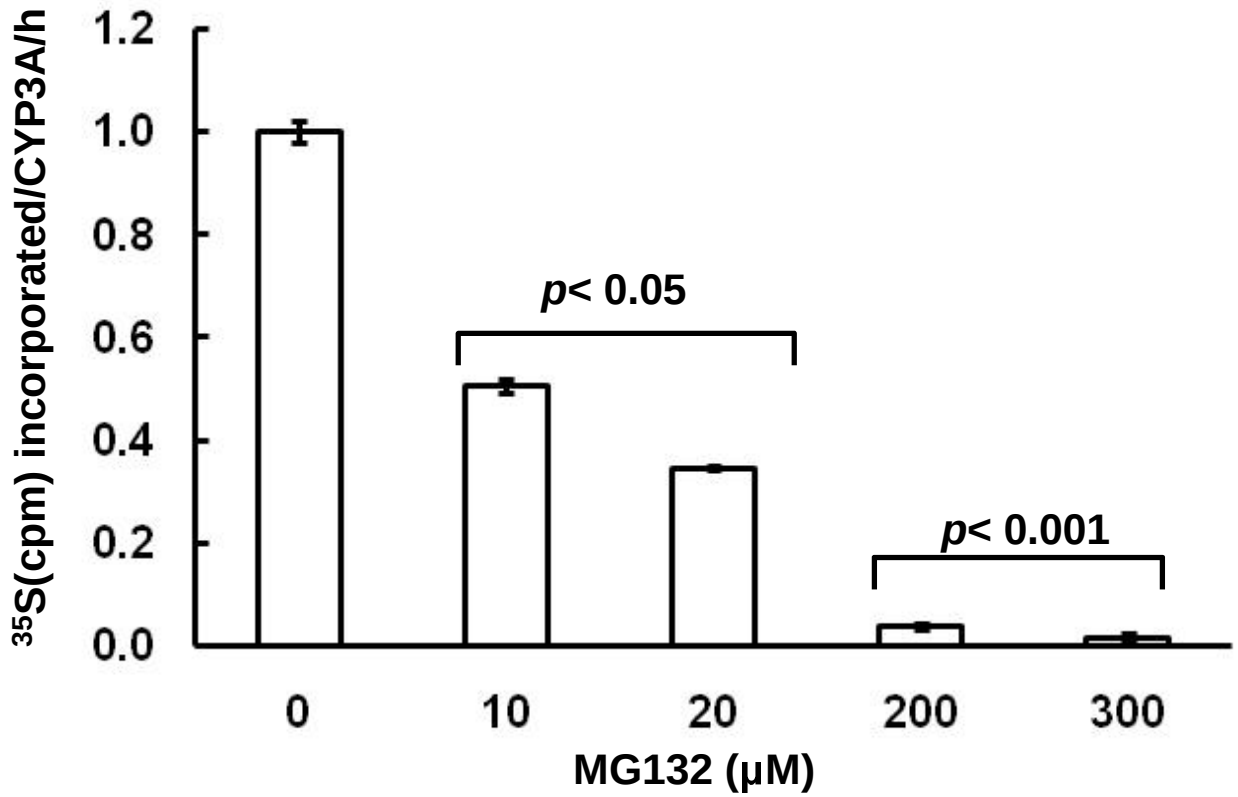

Figure 7

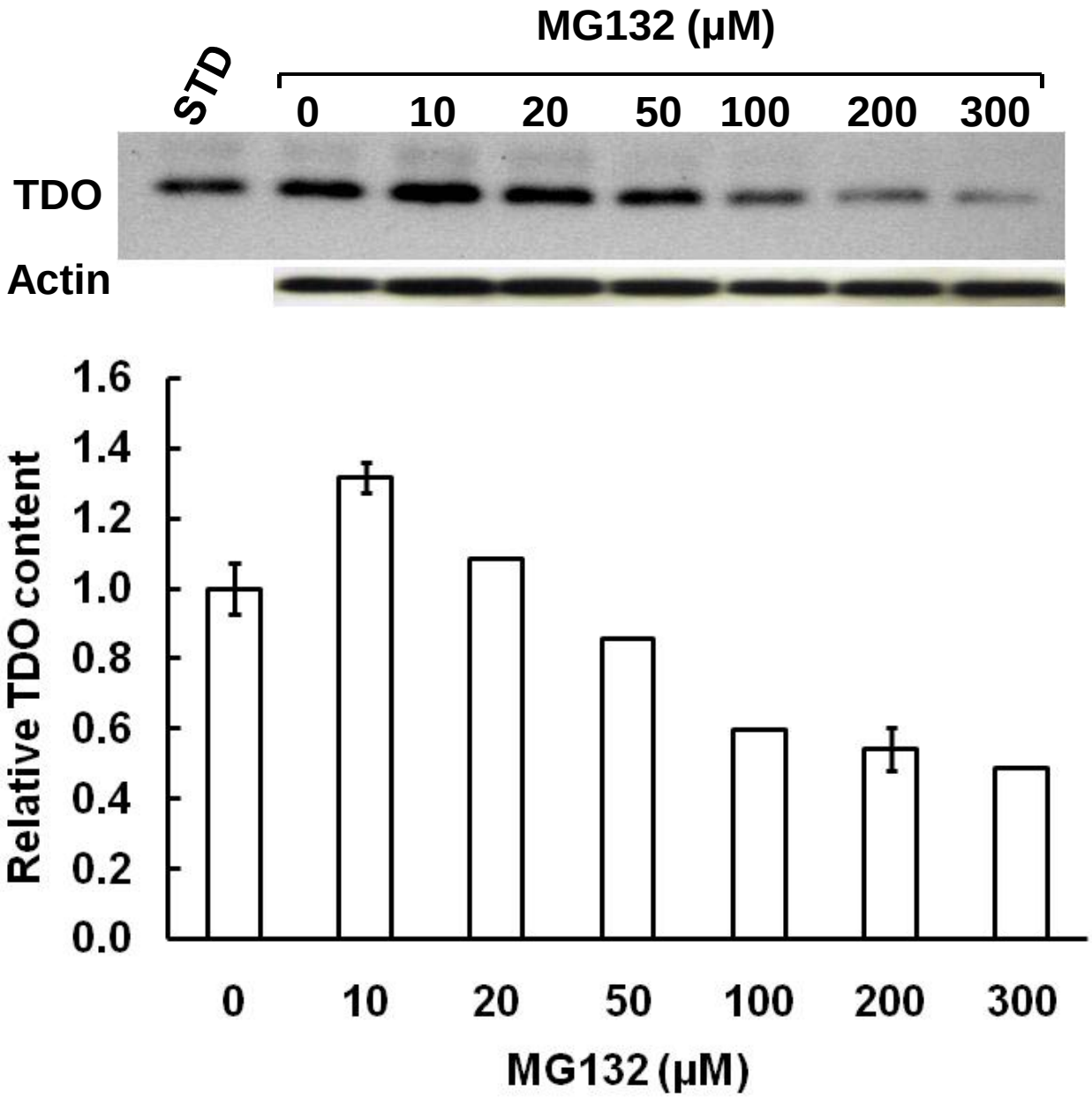

Figure 8

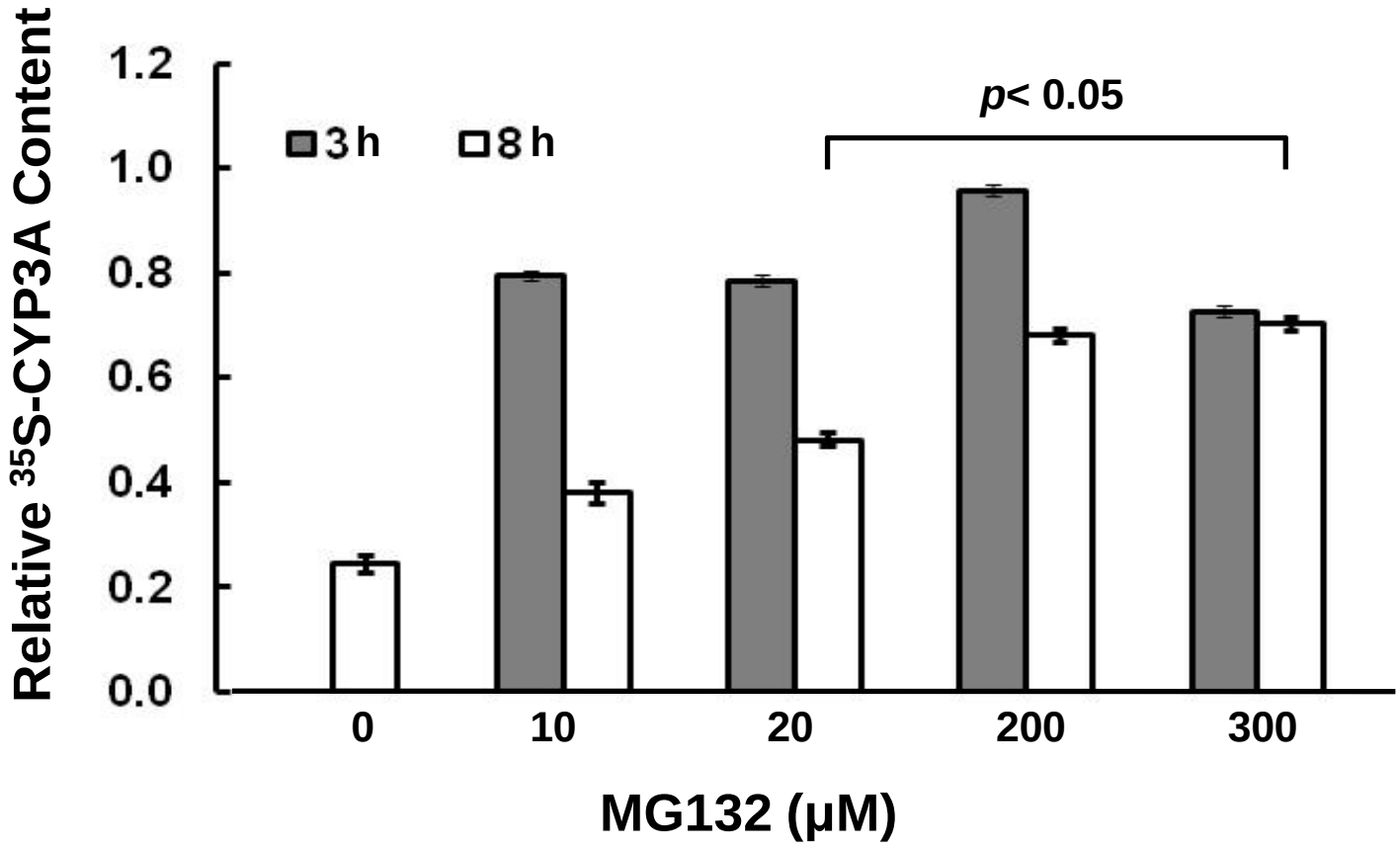

Figure 9

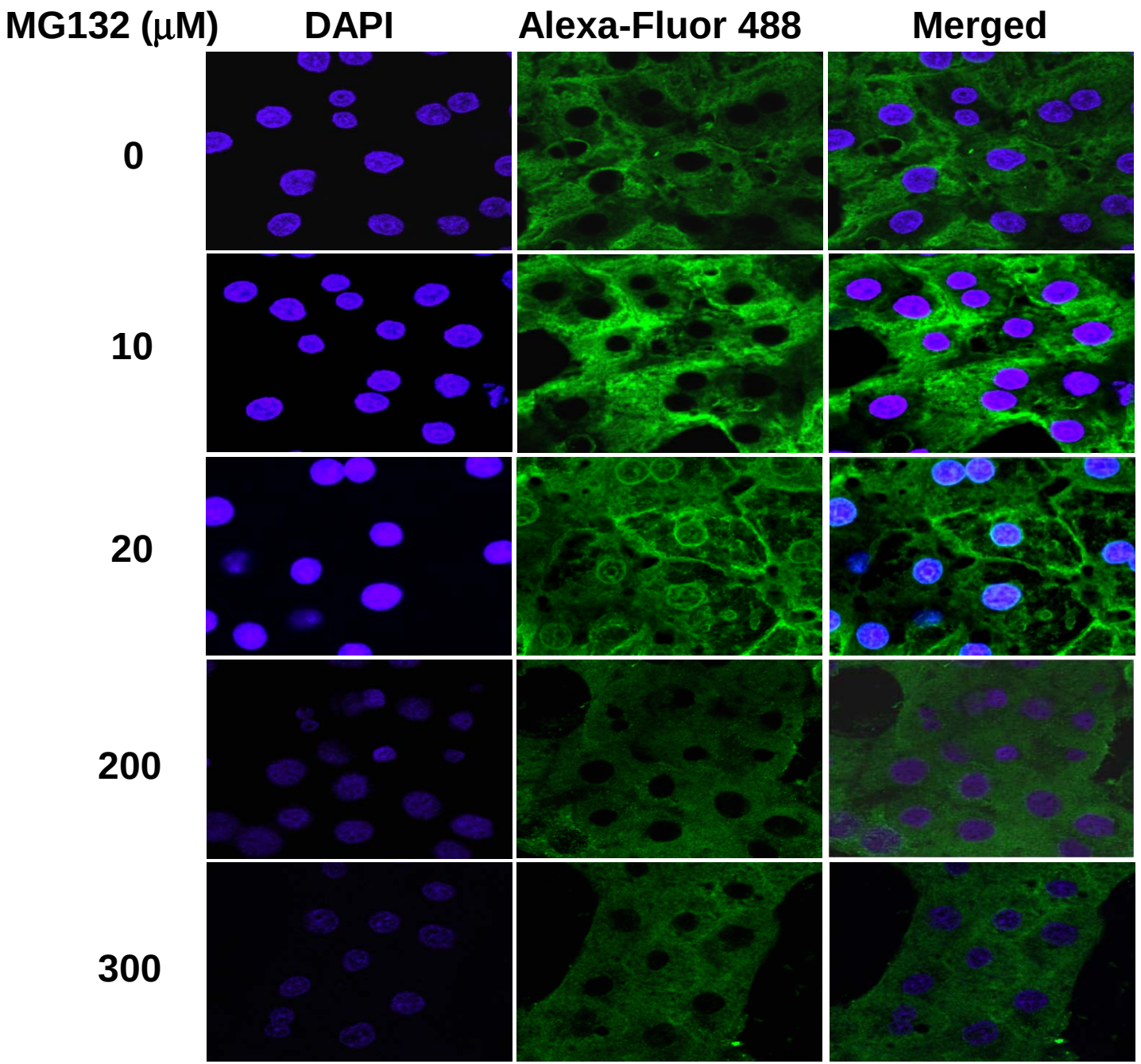

Figure 10A

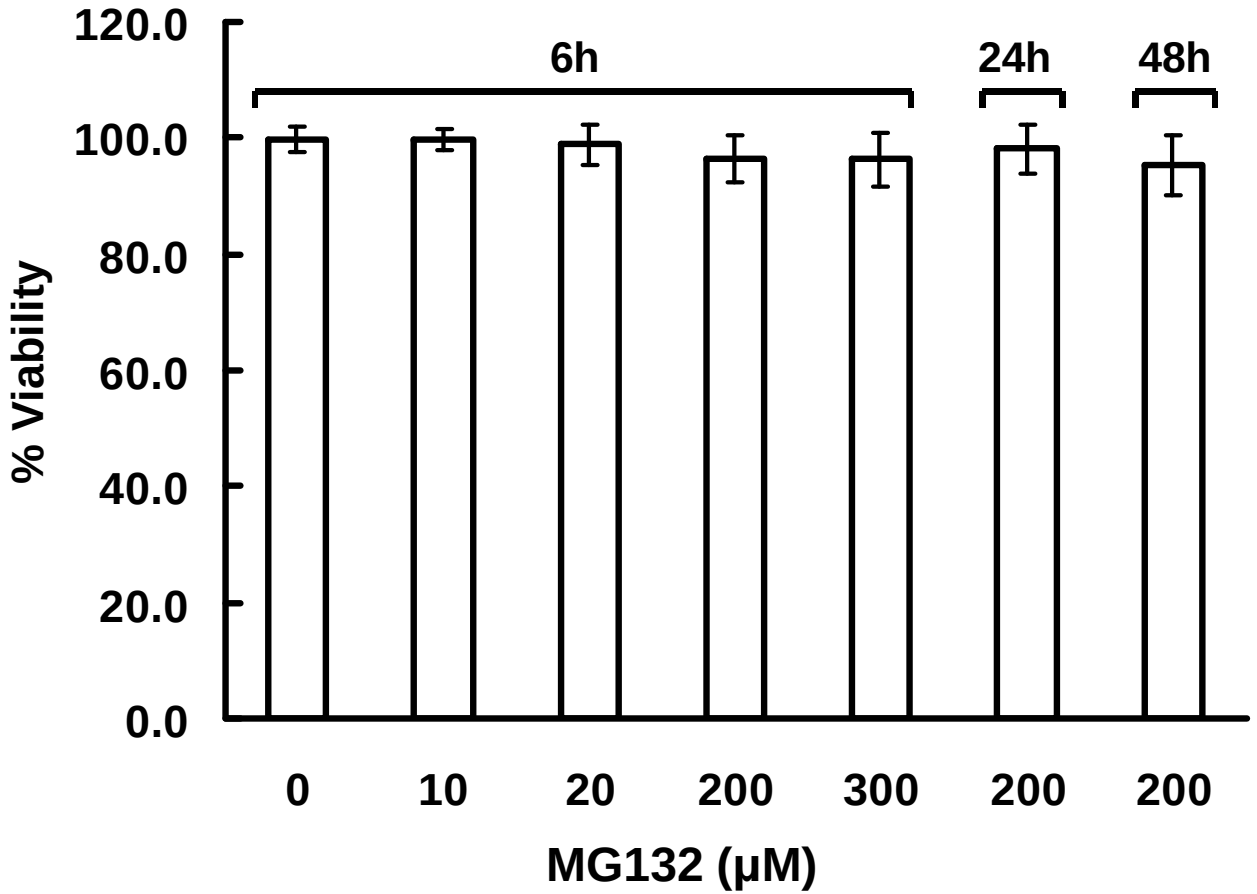

Figure 10B

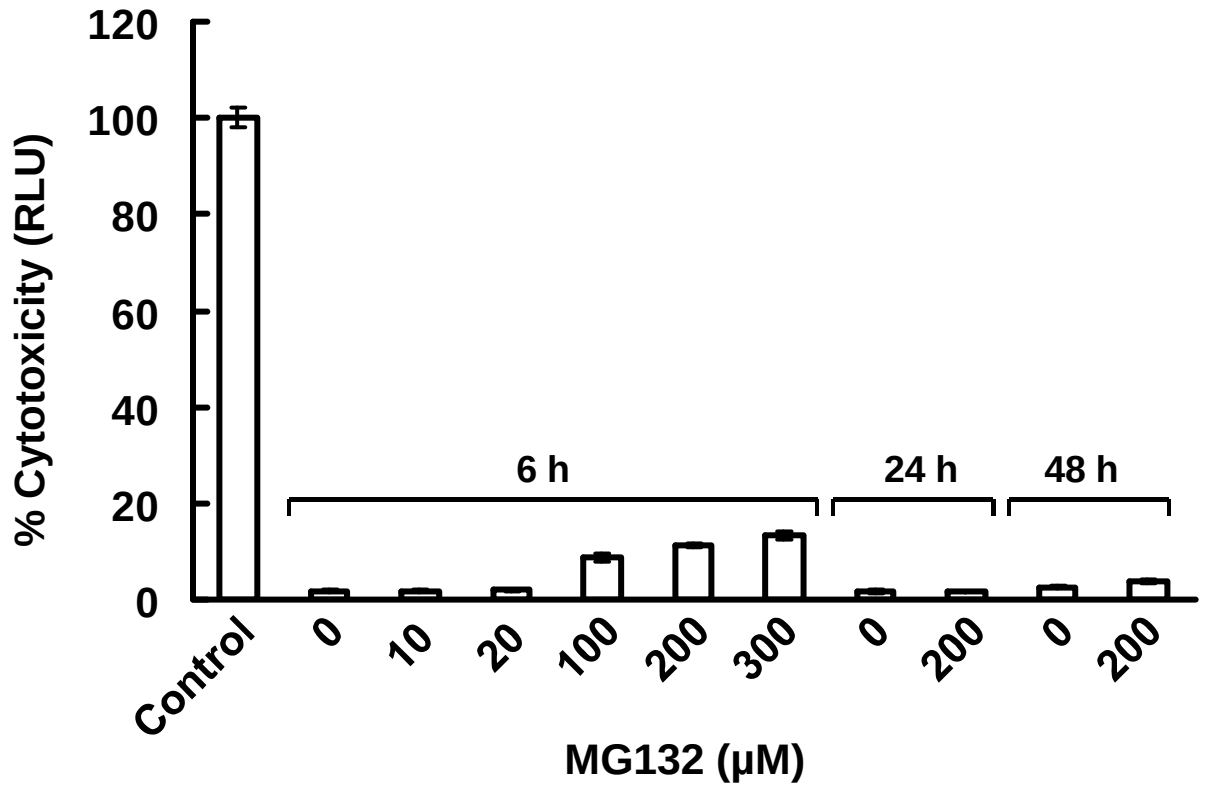

Figure 10C